Journal of Molecular and Cellular Cardiology 77 (2014) 29–41

Contents lists available at ScienceDirect

Journal of Molecular and Cellular Cardiology

journal homepage: www.elsevier.com/locate/yjmcc

Original article

Development of an experimentally useful model of acute myocardial infarction: 2/3 nephrectomized triple nitric oxide synthases-deficient mouse

Taro Uchida [a,1], Yumi Furuno [b,1], Akihide Tanimoto [c], Yumiko Toyohira [d], Kumiko Arakaki [e], Mika Kina-Tanada [a], Haruaki Kubota [a], Mayuko Sakanashi [a], Toshihiro Matsuzaki [a], Katsuhiko Noguchi [a], Junko Nakasone [a], Tomonori Igarashi [f], Susumu Ueno [f], Masayuki Matsushita [g], Shogo Ishiuchi [h], Hiroaki Masuzaki [i], Yusuke Ohya [e], Nobuyuki Yanagihara [d], Hiroaki Shimokawa [j], Yutaka Otsuji [b], Masahito Tamura [b], Masato Tsutsui [a,*]

[a] Department of Pharmacology, Graduate School of Medicine, University of the Ryukyus, Okinawa, Japan
[b] Second Department of Internal Medicine, School of Medicine, Institute of Industrial Ecological Sciences, University of Occupational and Environmental Health, Kitakyushu, Japan
[c] Department of Pathology, Kagoshima University Graduate School of Medical and Dental Sciences, Kagoshima, Japan
[d] Department of Pharmacology, School of Medicine, Institute of Industrial Ecological Sciences, University of Occupational and Environmental Health, Kitakyushu, Japan
[e] Third Department of Internal Medicine, Graduate School of Medicine, University of the Ryukyus, Okinawa, Japan
[f] Department of Occupational Toxicology, Institute of Industrial Ecological Sciences, University of Occupational and Environmental Health, Kitakyushu, Japan
[g] Department of Physiology, Graduate School of Medicine, University of the Ryukyus, Okinawa, Japan
[h] Department of Neurosurgery, Graduate School of Medicine, University of the Ryukyus, Okinawa, Japan
[i] Second Department of Internal Medicine, Graduate School of Medicine, University of the Ryukyus, Okinawa, Japan
[j] Department of Cardiovascular Medicine, Tohoku University Graduate School of Medicine, Sendai, Japan

ARTICLE INFO

Article history:
Received 23 July 2014
Received in revised form 9 September 2014
Accepted 17 September 2014
Available online 28 September 2014

Keywords:
Arteriosclerosis
Acute myocardial infarction
Nitric oxide synthase
Sudden cardiac death

ABSTRACT

We investigated the effect of subtotal nephrectomy on the incidence of acute myocardial infarction (AMI) in mice deficient in all three nitric oxide synthases (NOSs). Two-thirds nephrectomy (NX) was performed on male triple NOSs$^{-/-}$ mice. The 2/3NX caused sudden cardiac death due to AMI in the triple NOSs$^{-/-}$ mice as early as 4 months after the surgery. The 2/3NX triple NOSs$^{-/-}$ mice exhibited electrocardiographic ST-segment elevation, reduced heart rate variability, echocardiographic regional wall motion abnormality, and accelerated coronary arteriosclerotic lesion formation. Cardiovascular risk factors (hypertension, hypercholesterolemia, and hyperglycemia), an increased number of circulating bone marrow-derived vascular smooth muscle cell (VSMC) progenitor cells (a pro-arteriosclerotic factor), and cardiac up-regulation of stromal cell-derived factor (SDF)-1α (a chemotactic factor of the progenitor cells) were noted in the 2/3NX triple NOSs$^{-/-}$ mice and were associated with significant increases in plasma angiotensin II levels (a marker of renin–angiotensin system activation) and urinary 8-isoprostane levels (a marker of oxidative stress). Importantly, combined treatment with a clinical dosage of an angiotensin II type 1 receptor blocker, irbesartan, and a calcium channel antagonist, amlodipine, markedly prevented coronary arteriosclerotic lesion formation and the incidence of AMI and improved the prognosis of those mice, along with ameliorating all those pro-arteriosclerotic parameters. The 2/3NX triple NOSs$^{-/-}$ mouse is a new experimentally useful model of AMI. Renin–angiotensin system activation, oxidative stress, cardiovascular risk factors, and SDF-1α-induced recruitment of bone marrow-derived VSMC progenitor cells appear to be involved in the pathogenesis of AMI in this model.

1. Introduction

Acute myocardial infarction is a disorder in which cardiac myocytes undergo necrosis as a consequence of interrupted coronary blood flow [1]. Acute myocardial infarction is a major cause of morbidity and mortality worldwide, with more than 7 million people in the world suffering from acute myocardial infarction each year [1]. Over the past two decades, the in-hospital mortality rate after admission for acute myocardial infarction has substantially declined to less than 10%, owing to

Abbreviations: ACE, angiotensin-converting enzyme; ADMA, asymmetric dimethylarginine; AMI, acute myocardial infarction; APC, activated protein C; apo E, apolipoprotein E; AT_1, angiotensin II type 1; CKD, chronic kidney disease; ECG, electrocardiography; FITC, fluorescein isothiocyanate; GAPDH, glyceraldehyde-3-phosphate dehydrogenase; HDL, high-density lipoprotein; mAb, monoclonal antibody; NO, nitric oxide; NOS, NO synthase; NX, nephrectomy; Sca-1$^+$, stem cell antigen-1$^+$; SDF-1α, stromal cell-derived factor-1α; VSMC, vascular smooth muscle cell; WHHL, Watanabe heritable hyperlipidemic; WT, wild-type.

* Corresponding author at: Department of Pharmacology, Graduate School of Medicine, University of the Ryukyus, 207 Uehara, Nishihara, Okinawa 903-0215, Japan. Tel.: +81 98 895 1133; fax: +81 98 895 1411.
E-mail address: tsutsui@med.u-ryukyu.ac.jp (M. Tsutsui).
[1] These authors contributed equally to this work.

http://dx.doi.org/10.1016/j.yjmcc.2014.09.021
0022-2828/

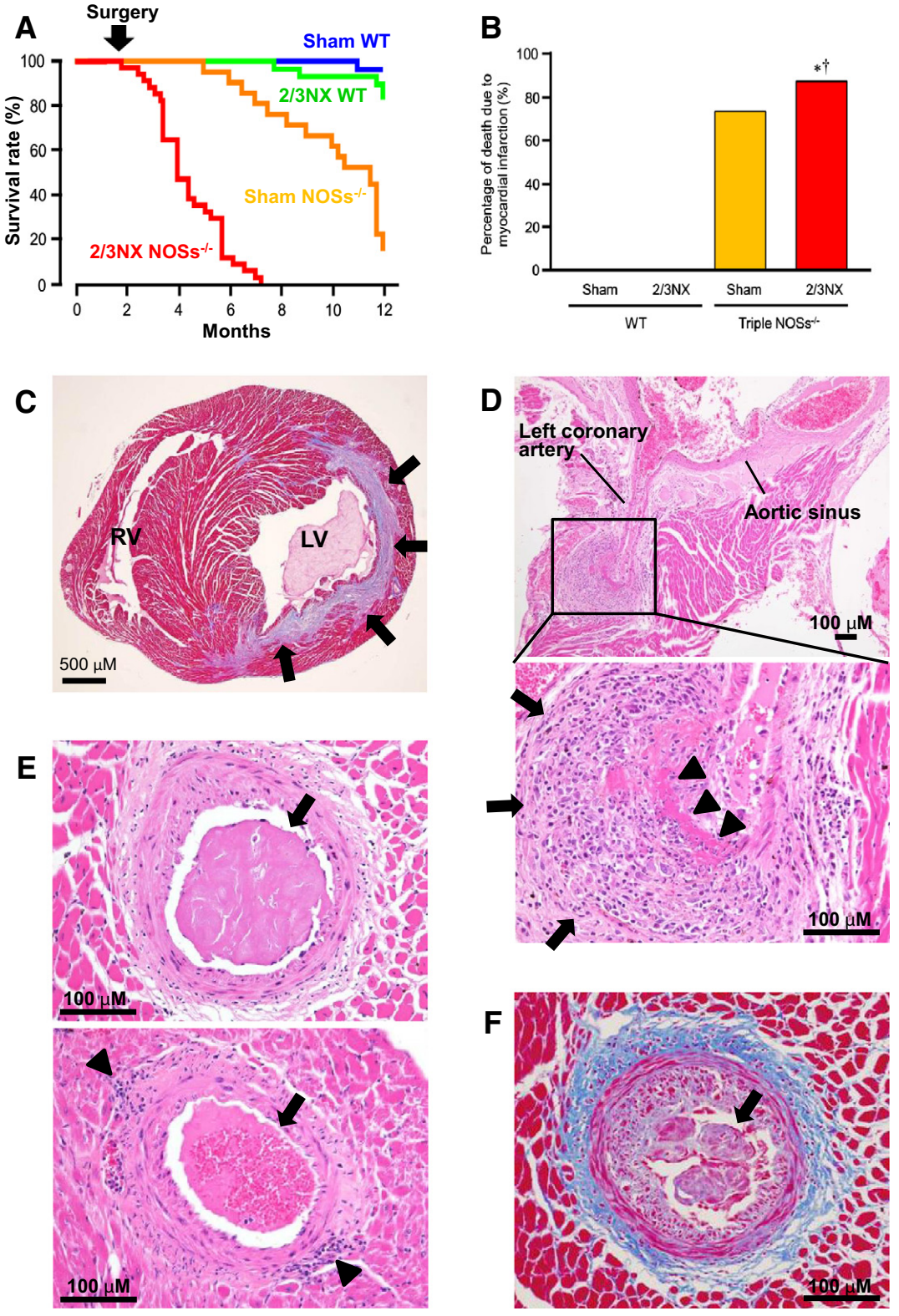

Fig. 1. Sudden cardiac death due to spontaneous myocardial infarction in 2/3 nephrectomized (NX) male triple nitric oxide synthases (NOSs)-deficient mice. (A) Survival rate ($n = 28$–49). NOSs$^{-/-}$, triple NOSs$^{-/-}$ mice; WT, wild-type mice; sham, sham-operated. (B) Percentage of death due to myocardial infarction in the total causes of death ($n = 2$–32). Sham, sham operation. (C) Lateral wall myocardial infarction (arrows) (Azan staining). LV, left ventricle; RV, right ventricle. (D) Marked infiltration of inflammatory cells (arrows) and fibrinoid necrosis (triangles) at the adventitia of the left coronary artery (hematoxylin-eosin staining). (E) Intracoronary thrombi (arrows) and adventitial infiltration of inflammatory cells (triangles) (hematoxylin–eosin staining). (F) Intimal thickening, perivascular fibrosis (blue color), and intracoronary thrombus (arrow) (Azan staining).

recent therapeutic advances such as coronary reperfusion therapy [2]. However, the overall mortality rate, including out-of-hospital deaths, is very high (approximately 30%) even at present [3]. This is because the majority of these deaths occur before stricken individuals reach the hospital [3]. Outside the hospital, once the individuals develop severe complications, such as malignant cardiac arrhythmia, cardiogenic shock, or cardiac rupture, it is extremely difficult to save their lives [3]. Thus, in order to suppress this fatal cardiovascular disorder, research and development of therapeutic strategies for preventing acute myocardial infarction are of critical importance. However, due to lack of an experimentally useful animal model that develops acute myocardial infarction, the research and development of such strategies have made little progress.

Nitric oxide (NO) plays an essential role in maintaining cardiovascular homeostasis. NO is synthesized by three distinct NO synthase (NOS) isoforms, including neuronal, inducible, and endothelial NOSs, and exerts a variety of biological actions under both physiological and pathological conditions [4–9]. We previously generated mice in which all three NOS genes are completely disrupted [10] and reported that triple NOSs$^{-/-}$ mice, but not single endothelial NOS$^{-/-}$ mice, spontaneously emerge acute myocardial infarction [11]. However, our model was not useful for experiments because it took a very long time (approximately 1 year) for them to develop acute myocardial infarction [11].

Chronic kidney disease (CKD) is a condition characterized by progressive and irreversible loss of renal function. It is estimated that over 10% of the adult population in developed countries suffer some degree of CKD [12,13]. Previous epidemiological studies have indicated that the presence of CKD significantly increases the risk of acute myocardial infarction in men, and that the impact of CKD on the risk of cardiovascular disease is as strong as that of diabetes mellitus and pre-existing ischemic heart disease [14–16]. In the clinical course of the progression of CKD, the number of nephrons decreases regardless of etiology, and this pathological renal remodeling is thought to be the final common

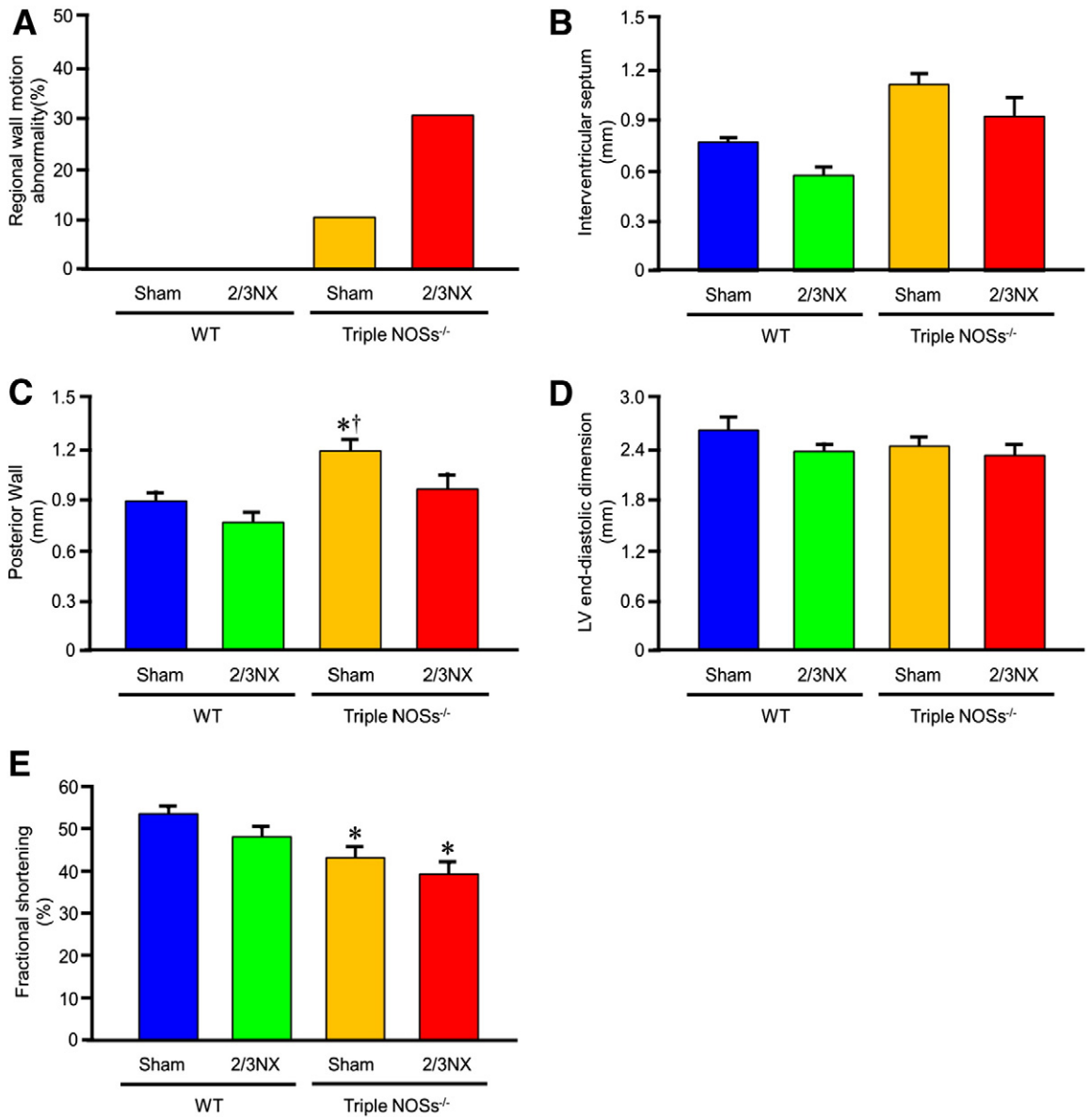

Fig. 2. Echocardiographic abnormalities in 2/3NX triple NOSs$^{-/-}$ mice at 2 months after the surgery. (A) Regional wall motion abnormality ($n = 10$). NOSs$^{-/-}$, triple NOSs$^{-/-}$ mice; WT, wild-type mice; sham, sham-operated. (B) Wall thickness of interventricular septum ($n = 10$). (C) Wall thickness of posterior wall ($n = 10$). (D) Left ventricular (LV) end-diastolic dimension ($n = 10$), (E) Fractional shortening ($n = 10$).

pathway in the pathogenesis of CKD. Such a disease state is modeled in experimental animals by surgically dissecting a large part of the renal mass [17,18].

In the present study, based on these backgrounds, we investigated the effect of subtotal nephrectomy on the incidence of acute myocardial infarction in our male triple NOSs$^{-/-}$ mice in order to establish an experimentally useful model of acute myocardial infarction.

2. Materials and methods

Materials and methods are described in the online Supplementary Methods and Results.

3. Results

3.1. Subtotal 2/3 nephrectomy (NX) caused an early onset of acute myocardial infarction in male triple NOSs$^{-/-}$ mice

Because animals with 5/6NX are widely used as an experimental model of CKD, we first studied the effect of 5/6NX on survival rate in male triple NOSs$^{-/-}$ mice. However, almost all the triple NOSs$^{-/-}$ mice died shortly after the 5/6NX (data not shown). Thus, we next examined the effect of 2/3NX. In male wild-type (WT) mice, the 2/3NX did not significantly affect the survival rate as compared with sham operation, and more than 80% of the 2/3NX WT mice lived during the 10 months of follow-up (Fig. 1A). In contrast,

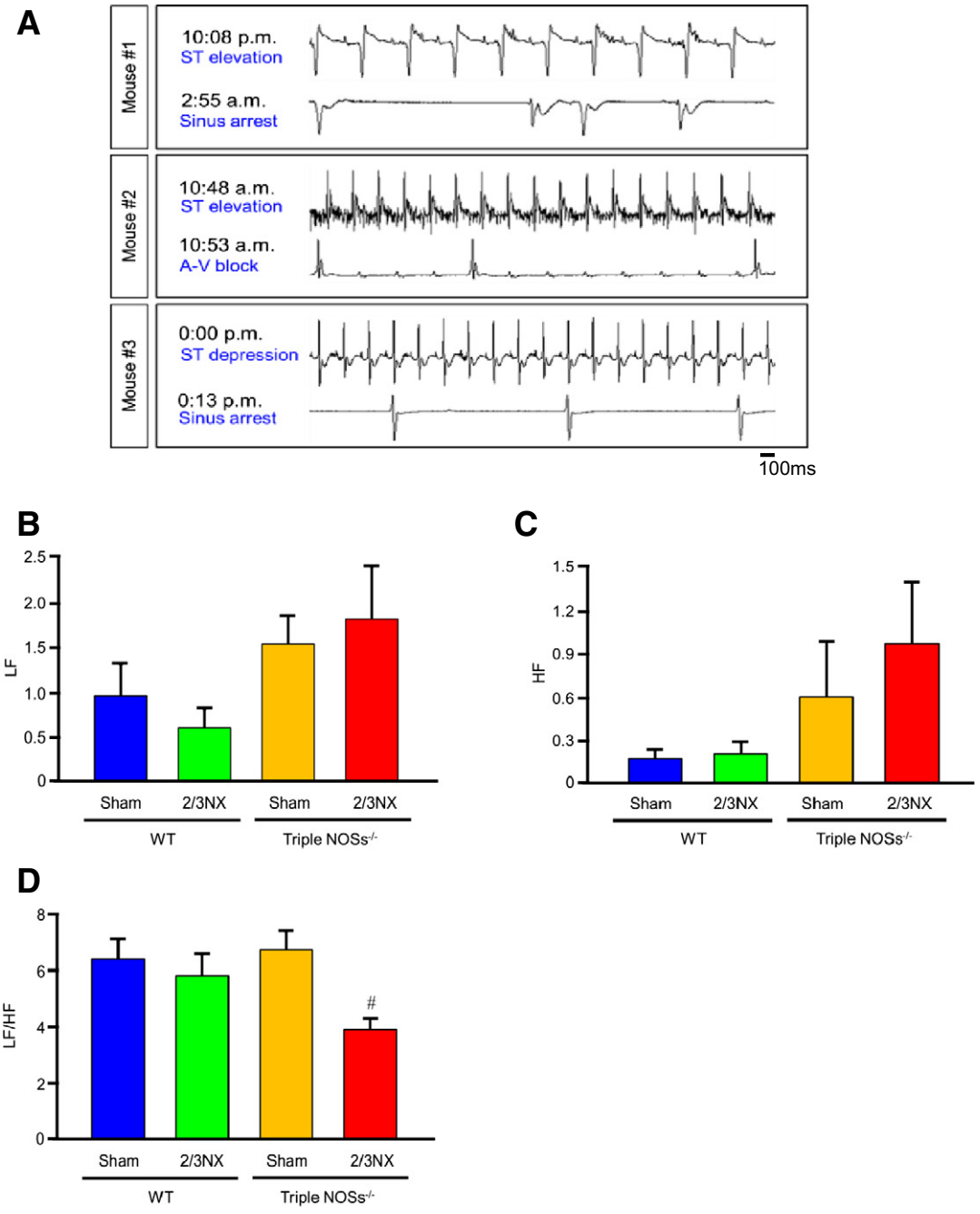

Fig. 3. Telemetry electrocardiographic abnormalities in 2/3NX triple NOSs$^{-/-}$ mice at 2 months after the surgery. (A) Electrocardiographic (ECG) abnormalities in 3 2/3NX triple NOSs$^{-/-}$ mice that died during ECG recording (died within 24 hours after subcutaneous implantation of telemetry transmitters). A-V, atrioventricular. (B) Low-frequency (LF) power ($n = 10$–12). (C) High-frequency (HF) power ($n = 10$–12). (D) LF/HF ratio ($n = 10$–12). $^{*}P < 0.05$ vs. sham-operated WT mice; $^{\#}P < 0.05$ vs. sham-operated triple NOSs$^{-/-}$ mice.

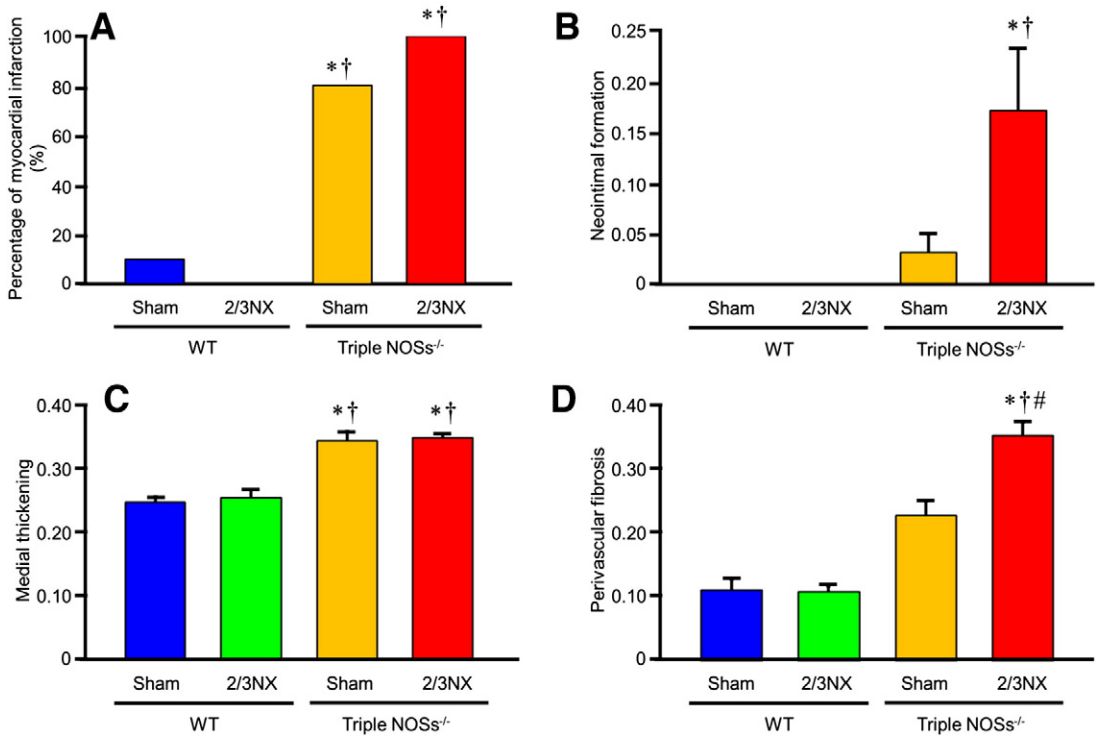

Fig. 4. Coronary arteriosclerotic lesion formation in 2/3NX triple NOSs$^{-/-}$ mice at 2 months after the surgery. After the echocardiography and telemetry ECG, pathological examination of the heart was performed. Four 2/3NX triple NOSs$^{-/-}$ mice that died before 2 months after the surgery and 3 2/3NX triple NOSs$^{-/-}$ mice that died during telemetry ECG were included in the analysis. The heart was cut into 5 equal-thick parts in a short-axis direction, and respective 5 sections were examined. (A) Percentage of acute and/or old myocardial infarction (n = 10–16). NOSs$^{-/-}$, triple NOSs$^{-/-}$ mice; WT, wild-type mice; sham, sham-operated. (B) Neointimal formation (the ratio of intima area to media area) (n = 10–16). (C) Medial thickening (the ratio of media area to total vascular area) (n = 10–16). (D) Perivascular fibrosis (the ratio of perivascular area to total vascular area) (n = 10–16). $^{*}P < 0.05$ vs. sham-operated WT mice; $^{\dagger}P < 0.05$ vs. 2/3NX WT mice; $^{\#}P < 0.05$ vs. sham-operated triple NOSs$^{-/-}$ mice.

in the triple NOSs$^{-/-}$ mice, the 2/3NX significantly and markedly reduced the survival rate compared with sham operation, and, importantly, approximately 90% of the 2/3NX triple NOSs$^{-/-}$ mice suddenly died as early as 4 months after the surgery (Fig. 1A).

We next explored the effect of 2/3NX on the incidence of acute myocardial infarction in the triple NOSs$^{-/-}$ mice by a postmortem examination, which revealed a marked increase in the incidence of myocardial infarction (the percentage of death due to myocardial infarction in the total causes of death) compared with sham operation. Noticeably, 87.8% (43/49) of the 2/3NX triple NOSs$^{-/-}$ mice died due to acute and/or old myocardial infarction (Fig. 1B). It was conceivable that the 2/3NX triple NOSs$^{-/-}$ mice would die mainly due to myocardial infarction-complicated arrhythmias or heart failure (including cardiogenic shock). It is difficult to distinguish between death due to arrhythmias and heart failure since heart failure is often accompanied by arrhythmias and since arrhythmias are always seen prior to any death. Thus, we categorized those causes of death as death due to myocardial infarction. No cerebrovascular disease was observed in any of the dead 2/3NX triple NOSs$^{-/-}$ mice. Fig. 1C represents the lateral wall myocardial infarction seen in the dead 2/3NX triple NOSs$^{-/-}$ mice. The coronary arteries of the dead 2/3NX triple NOSs$^{-/-}$ mice exhibited severe coronary arteriosclerotic lesion formation, including infiltration of inflammatory cells (Fig. 1D), neointimal formation (Fig. 1F), medial thickening (Fig. 1F), perivascular fibrosis (Fig. 1F), and fibrinoid necrosis (Fig. 1D), as well as coronary thrombus formation (Figs. 1E, F). On the other hand, coronary atherosclerotic lesions, such as extracellular lipid accumulation, atheromatous plaque formation, or infiltration of foamy macrophages in the coronary artery, were rarely observed.

3.2. 2/3NX caused echocardiographic and electrocardiographic abnormalities and accelerated coronary arteriosclerotic lesion formation in triple NOSs$^{-/-}$ mice at 2 months after the surgery

We then examined cardiac functional abnormalities and the extent of coronary arteriosclerotic lesion formation in the 2/3NX triple NOSs$^{-/-}$ mice at 2 months post-surgery via echocardiography, telemetry electrocardiography (ECG), and pathological examination. Of the 16 2/3NX triple NOSs$^{-/-}$ mice, 4 died before 2 months after the surgery. Echocardiography showed regional wall motion abnormality in 30% (3/10) of the 2/3NX triple NOSs$^{-/-}$ mice and 10% (1/10) of the sham triple NOSs$^{-/-}$ mice (Fig. 2A). Wall thickness of interventricular septum and posterior wall tended to be thinner and fractional shortening tended to be more reduced in the 2/3NX triple NOSs$^{-/-}$ mice as compared with the sham triple NOSs$^{-/-}$ mice, and fractional shortening was significantly decreased in the 2/3NX triple NOSs$^{-/-}$ mice when compared with the sham WT mice (Figs. 2B, C, E). There was no significant difference in left ventricular end-diastolic dimension between the 2/3NX triple NOSs$^{-/-}$ mice and other mice (Fig. 2D).

Of the 12 2/3NX triple NOSs$^{-/-}$ mice that received subcutaneous implantation of telemetry transmitters, 3 died during ECG recording (within 24 hours after the implantation), and ECG revealed ST-segment elevation followed by sinus arrest, ST-segment elevation followed by advanced atrioventricular block, and ST-segment depression followed by sinus arrest (Fig. 3A). Transient ST-segment depression was detected in other 2 2/3NX triple NOSs$^{-/-}$ mice and 1 sham triple NOSs$^{-/-}$ mice. No ischemic ECG change was seen in sham or 2/3NX WT mice. We evaluated heart rate variability parameters, such as low-frequency (LF) power, high-frequency (HF) power, and LF/HF ratio.

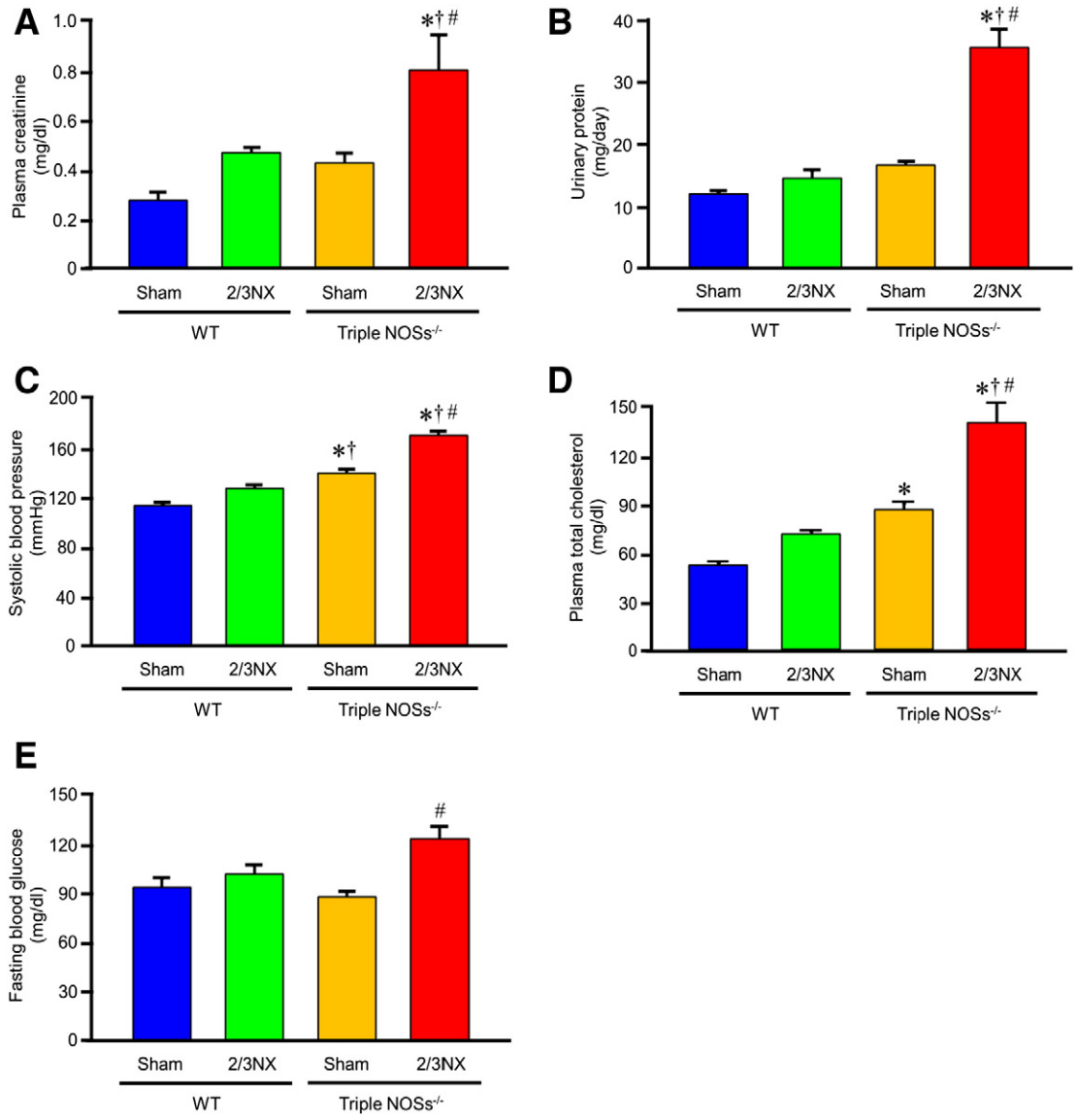

Fig. 5. Renal dysfunction and cardiovascular risk factors in the 2/3NX triple NOSs$^{-/-}$ mice. These parameters were assessed at 2 months after the surgery. (A) Plasma creatinine levels ($n = 10$). (B) Urinary protein levels ($n = 12$). (C) Systolic blood pressure ($n = 12$). (D) Plasma total cholesterol levels ($n = 10$). (E) Fasting blood glucose levels ($n = 10$). $^{*}P < 0.05$ vs. sham-operated WT mice; $^{\dagger}P < 0.05$ vs. 2/3NX WT mice; $^{\#}P < 0.05$ vs. sham-operated triple NOSs$^{-/-}$ mice.

The LF power and the HF power tended to be increased in the 2/3NX triple NOSs$^{-/-}$ mice, and the LF/HF ratio was significantly decreased in the 2/3NX triple NOSs$^{-/-}$ mice as compared with the sham NOSs$^{-/-}$ mice (Figs. 3B–D).

After echocardiography and telemetry ECG, we quantitated the extent of coronary arteriosclerosis. Four 2/3NX triple NOSs$^{-/-}$ mice that died before 2 months after the surgery and 3 2/3NX triple NOSs$^{-/-}$ mice that died during telemetry ECG were included in the analysis. The heart was cut into 5 equal-thick parts in a short-axis direction, and respective 5 sections were examined. Acute and/or old myocardial infarction was recognized in 100% (16/16) of the 2/3NX triple NOSs$^{-/-}$ mice and 80% (8/10) of the sham triple NOSs$^{-/-}$ mice (Fig. 4A). The extents of neointimal formation, medial thickening, and perivascular fibrosis were all markedly accelerated in the 2/3NX triple NOSs$^{-/-}$ mice as compared with the sham WT mice (Figs. 4B–D). Coronary thrombus formation was also noted in 1 2/3NX triple NOSs$^{-/-}$ mice.

3.3. 2/3NX reduced renal function in triple NOSs$^{-/-}$ mice

There were significant increases in plasma creatinine and urinary protein levels, markers of renal function, after the 2/3NX (assessed at 2 months after the surgery) in the triple NOSs$^{-/-}$ mice compared with sham operation (Figs. 5A, B).

Fig. 6. Stromal cell-derived factor (SDF)-1α-induced recruitment of circulating bone marrow-derived vascular smooth muscle cell (VSMC) progenitor cells, renin–angiotensin system activation, and oxidative stress in the 2/3NX triple NOS$^{-/-}$ mice. (A and B) The number of circulating stem cell antigen-1^{+} (Sca-1^{+})/c-Kit^{-}/Lin^{-} cells (interpreted as bone marrow-derived VSMC progenitor cells) analyzed at 1 week after the surgery ($n = 7$). (C) Cardiac SDF-1α protein levels assayed at 1 week after the surgery ($n = 4$–6). (D) Plasma angiotensin II levels measured at 2 months after the surgery ($n = 8$). (E) Cardiac angiotensin-converting enzyme (ACE) protein expression levels evaluated at 2 months after the surgery ($n = 7$). (F) Urinary 8-isoprostane levels assessed at 2 months after the surgery ($n = 8$). $^{*}P < 0.05$ vs. sham-operated WT mice; $^{\dagger}P < 0.05$ vs. 2/3NX WT mice; $^{\#}P < 0.05$ vs. sham-operated triple NOSs$^{-/-}$ mice.

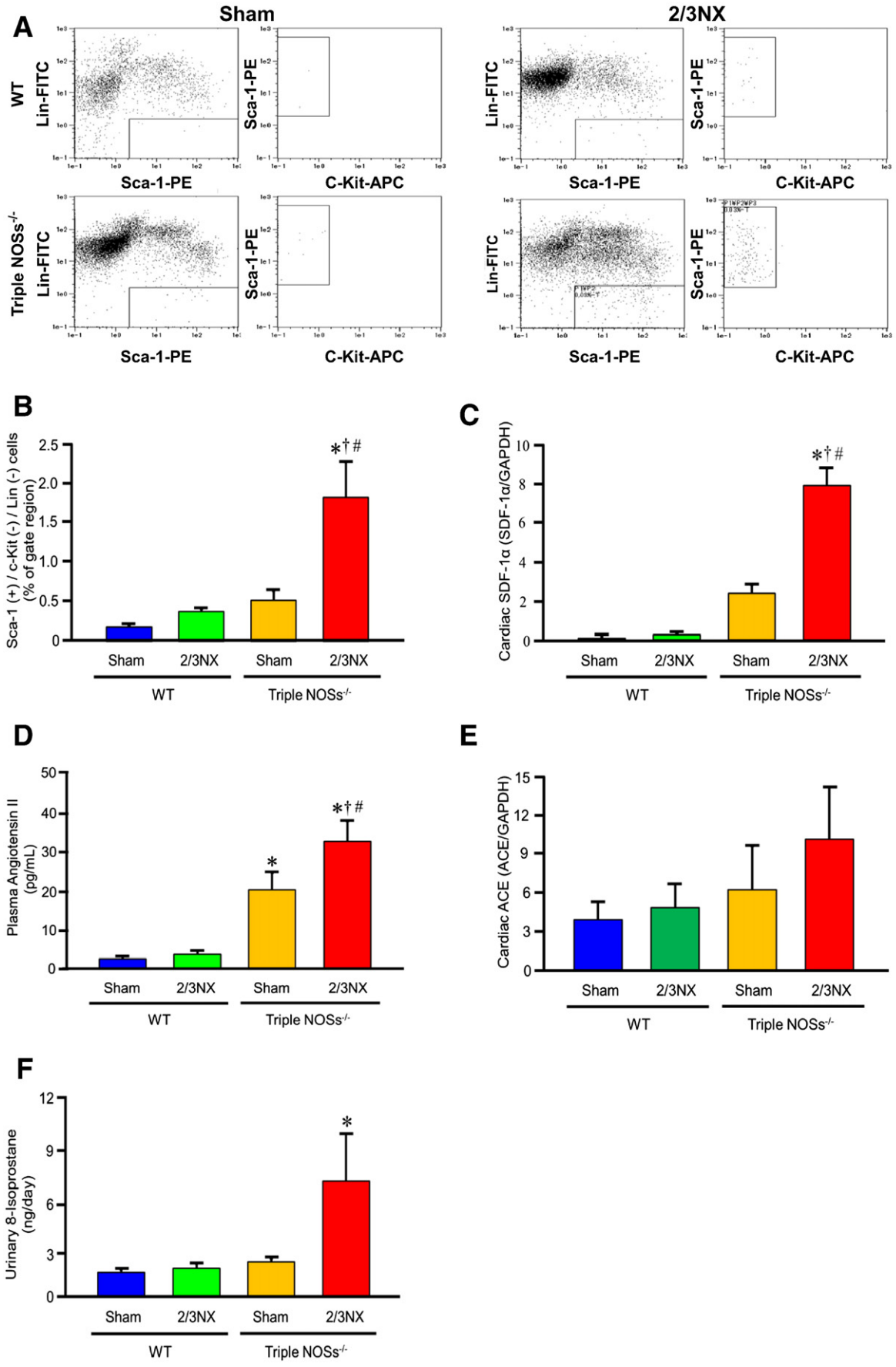
A
Sham
2/3NX
WT
Triple NOSs-/-
Lin-FITC
Sca-1-PE
C-Kit-APC
B
Sca-1 (+) / c-Kit (-) / Lin (-) cells (% of gate region)
C
Cardiac SDF-1α (SDF-1α/GAPDH)
D
Plasma Angiotensin II (pg/mL)
E
Cardiac ACE (ACE/GAPDH)
F
Urinary 8-Isoprostane (ng/day)
Sham
2/3NX
WT
Triple NOSs-/-

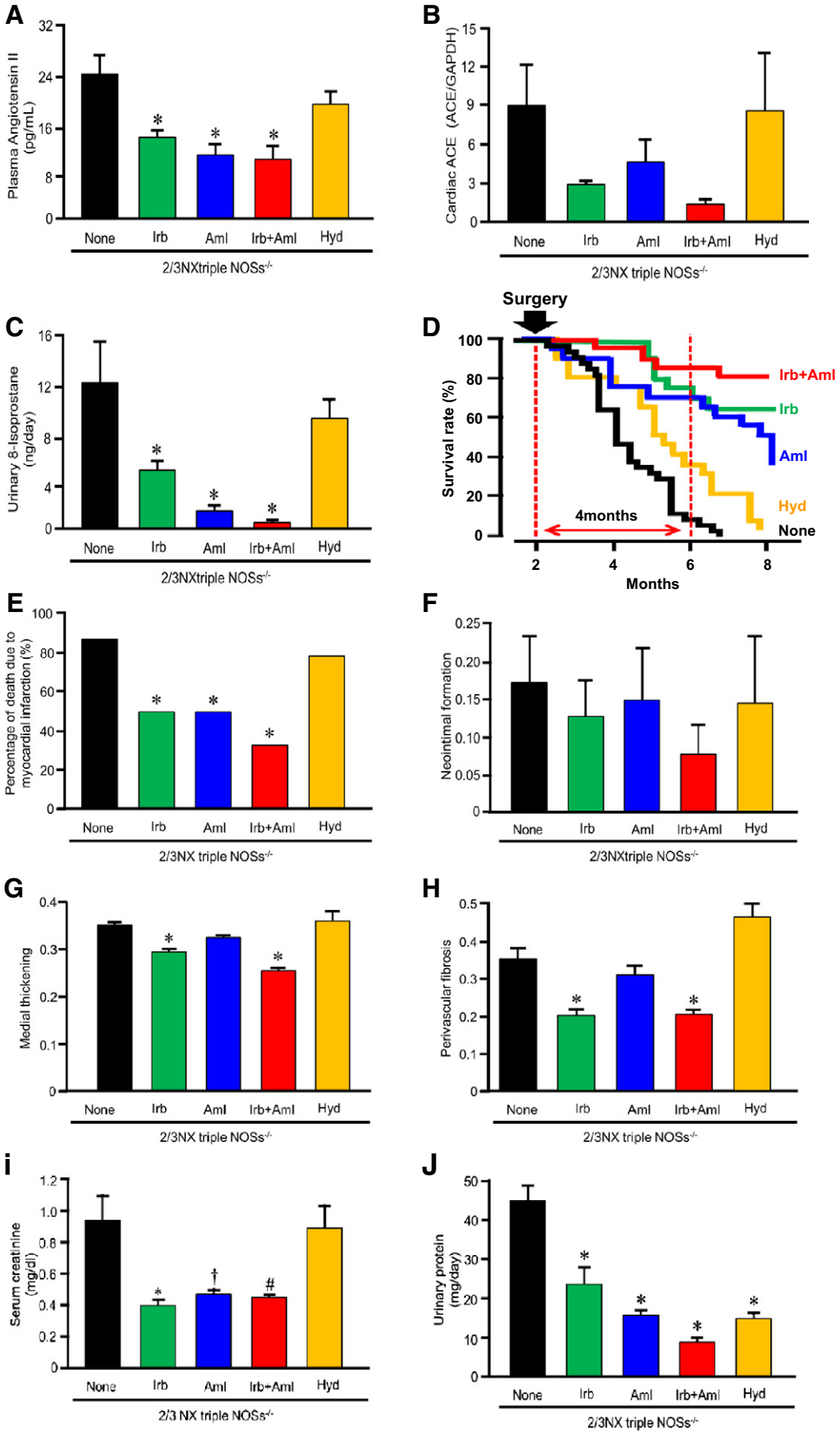
A
Plasma Angiotensin II (pg/mL)
None
Irb
Aml
Irb+Aml
Hyd
2/3NXtriple NOSs-/-
B
Cardiac ACE (ACE/GAPDH)
2/3NX triple NOSs-/-
C
Urinary 8-Isoprostane (ng/day)
D
Surgery
Survival rate (%)
Irb+Aml
Irb
Aml
Hyd
None
4months
Months
E
Percentage of death due to myocardial infarction (%)
F
Neointimal formation
G
Medial thickening
H
Perivascular fibrosis
i
Serum creatinine (mg/dl)
J
Urinary protein (mg/day)

3.4. 2/3NX exacerbated cardiovascular risk factors in triple NOSs$^{-/-}$ mice

Because severe coronary arteriosclerotic lesions were detected in the 2/3NX triple NOSs$^{-/-}$ mice, we then examined the presence or absence of cardiovascular risk factors. The 2/3NX caused significant increases in systolic blood pressure (measured at 1 month after the surgery), plasma total cholesterol levels, and fasting blood glucose levels (evaluated at 2 months after the surgery) in the triple NOSs$^{-/-}$ mice compared with sham operation (Figs. 5C–E).

3.5. 2/3NX caused mobilization of circulating bone marrow-derived vascular smooth muscle cell (VSMC) progenitor cells and up-regulation of cardiac stromal cell-derived factor 1α (SDF-1α) levels in triple NOSs$^{-/-}$ mice

It has been reported that bone marrow-derived VSMC progenitor cells contribute to arteriosclerotic lesion formation after vascular injury and that SDF-1α recruits the VSMC progenitor cells to vascular lesions [19]. We thus analyzed the effects of 2/3NX on the number of circulating bone marrow-derived VSMC progenitor cells and cardiac SDF-1α protein levels in the triple NOSs$^{-/-}$ mice. The 2/3NX significantly and markedly augmented the number of circulating stem cell antigen-1^{+} (Sca-1^{+})/c-Kit^{-}/Lin^{-} cells, which are interpreted as bone marrow-derived VSMC progenitor cells (evaluated at 1 week after the surgery), and the cardiac SDF-1α protein levels (assayed at 1 week after the surgery) in the triple NOSs$^{-/-}$ mice compared with sham operation (Figs. 6A–C and Online Supplementary Fig. I).

3.6. 2/3NX caused renin–angiotensin system activation and oxidative stress in triple NOSs$^{-/-}$ mice

We next investigated the molecular mechanisms for acute myocardial infarction caused by the 2/3NX in the triple NOSs$^{-/-}$ mice. The 2/3NX evoked prominent increases in plasma angiotensin II levels and cardiac angiotensin-converting enzyme (ACE) protein levels, markers of renin–angiotensin system activation (assessed at 2 months after the surgery) in the triple NOSs$^{-/-}$ mice compared with sham operation (Figs. 6D and E, and Online Supplementary Fig. II), although the values of the cardiac ACE protein levels did not reach a statistically significant level because of variations in the data. The 2/3NX also elicited a marked rise in urinary 8-isoprostane levels, a marker of oxidative stress (measured at 2 months after the surgery), in the triple NOSs$^{-/-}$ mice (Fig. 6F).

3.7. Combined treatment with an angiotensin II type 1 (AT_1) receptor blocker, irbesartan, and an antioxidant calcium channel antagonist, amlodipine, markedly prevented coronary arteriosclerotic lesion formation and the occurrence of myocardial infarction and improved the prognosis of 2/3NX triple NOSs$^{-/-}$ mice

Finally, in order to examine the involvement of renin–angiotensin system activation and oxidative stress in the pathogenesis of acute myocardial infarction in the 2/3NX triple NOSs$^{-/-}$ mice, and also in order to validate the experimental usefulness of this acute myocardial infarction model, we investigated the effects on the cardiovascular abnormalities in this model of treatment with a selective and potent AT_1 receptor blocker, irbesartan; an antioxidant dihydropyridine calcium channel antagonist, amlodipine; a combination of both; or an anti-hypertensive agent, hydralazine. We used the clinical therapeutic dosage of irbesartan and amlodipine. Single treatment with irbesartan or amlodipine markedly reduced the plasma angiotensin II levels, the cardiac ACE protein levels, and the urinary 8-isoprostane levels in the 2/3NX triple NOSs$^{-/-}$ mice, while the combined treatment with irbesartan and amlodipine more potently decreased those values (Figs. 7A–C and Online Supplementary Fig. III), although the data of the cardiac ACE protein levels again did not reach a statistically significant level owing to dispersion of the data (Fig. 7B and Online Supplementary Fig. III). Mono-treatment with irbesartan or amlodipine significantly improved the survival rate in the 2/3NX triple NOSs$^{-/-}$ mice, while the irbesartan/amlodipine co-treatment more powerfully ameliorated it. More importantly, these significant effects were noted within the short time of 4 months after the drug treatment, indicating the usefulness of this model for pharmacological studies (Fig. 7D). The sole treatment with irbesartan or amlodipine inhibited the incidence of myocardial infarction (the percentage of death due to myocardial infarction in the total causes of death) and coronary arteriosclerotic lesion formation (neointimal formation, medial thickening, and perivascular fibrosis) in the 2/3NX triple NOSs$^{-/-}$ mice, while the simultaneous treatment with irbesartan and amlodipine more intensely prevented both the incidence of myocardial infarction (Fig. 7E) and coronary lesion formation (Figs. 7F–H). On the other hand, although the treatment with hydralazine significantly lowered systolic blood pressure in the 2/3NX triple NOSs$^{-/-}$ mice to the same extent as the treatment with irbesartan plus amlodipine (Fig. 8A), it did not significantly affect the plasma angiotensin II levels, the cardiac ACE protein levels, the urinary 8-isoprostane levels, the survival rate, the incidence of myocardial infarction, or coronary lesion formation (Figs. 7A–H).

The treatments with irbesartan, amlodipine, and their combination significantly diminished the plasma creatinine levels and the urinary protein levels in the 2/3NX triple NOSs$^{-/-}$ mice (Figs. 7I, J). The treatment with hydralazine also significantly attenuated the urinary protein levels, whereas it had no effect on the plasma creatinine levels (Figs. 7I, J). These results suggest that the decrease in the plasma creatinine levels might have been related to the renal protective actions of the pharmacological agents, while the reduction in the urinary protein levels might have been associated with the lowering of renal intraglomerular pressure induced by these anti-hypertensives.

The plasma total cholesterol levels and the fasting blood glucose levels in the 2/3NX triple NOSs$^{-/-}$ mice tended to be lessened by the treatment with irbesartan or amlodipine, while statistically significant effects were noted only by the combined irbesartan/amlodipine treatment (Figs. 8B, C). Similarly, while the number of circulating Sca-1^{+}/c-Kit^{-}/Lin^{-} cells and the cardiac SDF-1α protein levels in the 2/3NX triple NOSs$^{-/-}$ mice tended to be suppressed by the irbesartan or amlodipine treatment, statistically significant effects were recognized exclusively by the simultaneous treatment with the two agents (Figs. 8D–F and Online Supplementary Fig. IV).

4. Discussion

The major novel findings of the present study are as follows: (i) 2/3NX caused sudden cardiac death due to acute myocardial infarction in male triple NOSs$^{-/-}$ mice as early as 4 months after the surgery. (ii) The 2/3NX triple NOSs$^{-/-}$ mice exhibited electrocardiographic ST-segment elevation, reduced heart rate variability, echocardiographic regional wall motion abnormality, and accelerated coronary

Fig. 7. Effects of treatment with an angiotensin II type 1 (AT1) receptor blocker, irbesartan; an antioxidant calcium channel antagonist, amlodipine; a combination of irbesartan and amlodipine; or an anti-hypertensive agent, hydralazine, on renin–angiotensin system activation, oxidative stress, survival rate, incidence of myocardial infarction, coronary arteriosclerotic lesion formation, and renal function in the 2/3NX triple NOSs$^{-/-}$ mice. Irb, irbesartan (50 mg/kg/day in chow); Aml, amlodipine (3.2 mg/kg/day in drinking water); Hyd, hydralazine (250 mg/mL in drinking water). The effects of the drugs on coronary lesion formation were assessed in the 2/3NX triple NOSs$^{-/-}$ mice at 2 months after the surgery. (A) Plasma angiotensin II levels ($n = 10$). (B) Cardiac ACE protein expression levels ($n = 7$). (C) Urinary 8-isoprostane levels ($n = 8$). (D) Survival rate ($n = 20$–49). (E) Percentage of death due to myocardial infarction in the total causes of death ($n = 6$–49). (F) Neointimal formation (the ratio of intima area to media area) ($n = 6$–16). (G) Medial thickening (the ratio of media area to total vascular area) ($n = 6$–16). (H) Perivascular fibrosis (the ratio of perivascular area to total vascular area) ($n = 6$–16). (I) Serum creatinine levels ($n = 10$). (J) Urinary protein levels ($n = 10$). $^{*}P < 0.05$ vs. none (untreated control).

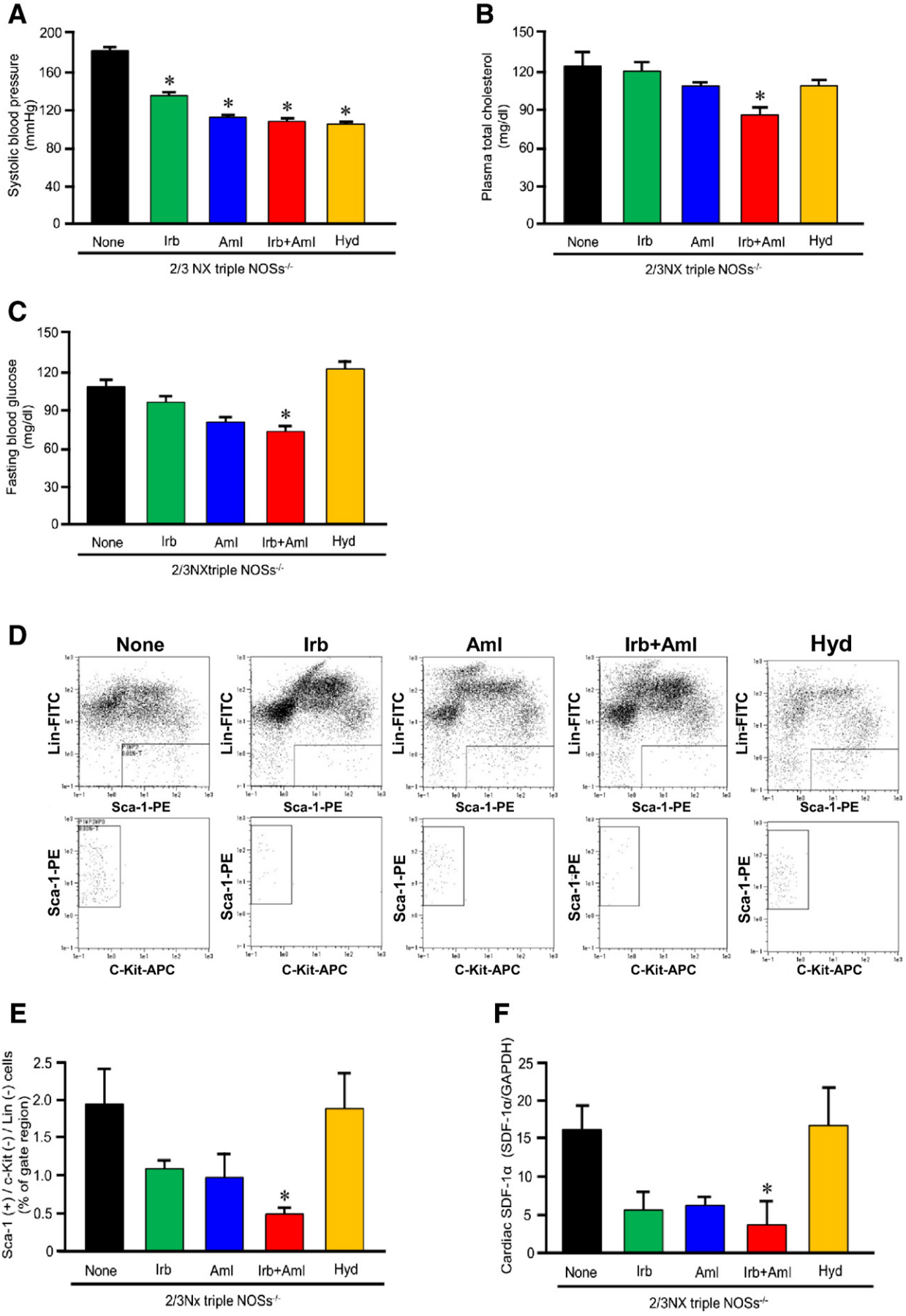
A
Systolic blood pressure (mmHg)
200
160
120
80
40
0
None
Irb
Aml
Irb+Aml
Hyd
2/3 NX triple NOSs-/-
B
Plasma total cholesterol (mg/dl)
150
120
90
60
30
0
None
Irb
Aml
Irb+Aml
Hyd
2/3NX triple NOSs-/-
C
Fasting blood glucose (mg/dl)
150
120
90
60
30
0
None
Irb
Aml
Irb+Aml
Hyd
2/3NXtriple NOSs-/-
D
None
Irb
Aml
Irb+Aml
Hyd
Lin-FITC
Sca-1-PE
C-Kit-APC
E
Sca-1 (+) / c-Kit (-) / Lin (-) cells (% of gate region)
2.5
2.0
1.5
1.0
0.5
0
None
Irb
Aml
Irb+Aml
Hyd
2/3Nx triple NOSs-/-
F
Cardiac SDF-1α (SDF-1α/GAPDH)
25
20
15
10
5
0
None
Irb
Aml
Irb+Aml
Hyd
2/3NX triple NOSs-/-

arteriosclerotic lesion formation. (iii) Cardiovascular risk factors (hypertension, hypercholesterolemia, and hyperglycemia), an increased number of circulating bone marrow-derived VSMC progenitor cells, and cardiac up-regulation of SDF-1α were noted in the 2/3NX triple NOSs$^{-/-}$ mice and were associated with significant increases in plasma angiotensin II levels and urinary 8-isoprostane levels. (iv) Simultaneous treatment with a clinical dosage of an angiotensin II type 1 receptor blocker, irbesartan, and an antioxidant calcium channel antagonist, amlodipine, markedly prevented coronary arteriosclerotic lesion formation and the incidence of myocardial infarction and improved the prognosis of those mice, along with ameliorating all those pro-arteriosclerotic parameters. Here we report the establishment of a new experimentally useful model of acute myocardial infarction.

4.1. Animal models that develops acute myocardial infarction

Five animal models that emerge acute myocardial infarction have thus far been reported. The first reported acute myocardial infarction model is a rat treated with a non-selective NOS inhibitor, such as N^{ω}-nitro-L-arginine methyl ester (L-NAME) or N^{ω}-nitro-L-arginine (L-NNA), chronically [20–23]. However, we clarified that arteriosclerotic vascular lesion formation caused by long-term treatment with L-NAME or L-NNA is not mediated by simple inhibition of NOSs activities [24]. While L-NAME- or L-NNA-treated rat shows multiple small infarcts without sudden death, those findings are quite different from human pathologies. The L-NAME- or L-NNA-treated rat has not been used at al as an acute myocardial infarction model. The second generated acute myocardial infarction model is the mouse with homozygous null mutations in the genes for both the high-density lipoprotein (HDL) receptor SR-B1 and apolipoprotein (apo) E [25]. The SR-B1$^{-/-}$/apoE$^{-/-}$ mouse dies of acute myocardial infarction before 2 months of age (in childhood) even when fed a standard chow diet [25]. This short-term occurrence of acute myocardial infarction would be useful for experiments. However, the clinical course in human patients with acute myocardial infarction, which usually occurs in adulthood, is different from the natural course in the SR-B1$^{-/-}$/apoE$^{-/-}$ mouse. The third produced model is the myocardial infarction-prone Watanabe heritable hyperlipidemic (WHHLMI) rabbit. The WHHLMI rabbit is not useful for experiments either because it takes a very long time (1 to 3 years) to develop acute myocardial infarction. The fourth created model is the SR-B1$^{-/-}$/hypomorphic apo ER61 (apoER$^{h/h}$) mouse, which shows high-fat diet-induced acute myocardial infarction [26]. Although the SR-B1$^{-/-}$/apoER$^{h/h}$ mouse may be a good model, it has not been used at all in experiments in which the effects of drugs or therapies are examined since its generation was published 9 years ago, and only one article with this mouse has been published after the generation [27]. We reported a fifth model, the triple NOSs$^{-/-}$ mouse, that spontaneously develops acute myocardial infarction. Unfortunately, however, it takes a very long time (approximately 1 year) for acute myocardial infarction to occur in our mouse. In the present study, the majority of the 2/3NX triple NOSs$^{-/-}$ mice exhibited sudden cardiac death due to acute myocardial infarction within as little as 4 months after the surgery, and the experimental usefulness of this model was validated by demonstrating the preventive effects of the combined treatment with irbesartan and amlodipine on the occurrence of acute myocardial infarction. Therefore, our 2/3NX triple NOSs$^{-/-}$ mouse is a new experimentally useful model of acute myocardial infarction.

Severe coronary arteriosclerosis, including infiltration of inflammatory cells, neointimal formation, medial thickening, and perivascular fibrosis, as well as coronary thrombus formation, was noted in the 2/3NX triple NOSs$^{-/-}$ mice. These findings closely resemble the human pathology seen in the infarct-related coronary arteries in patients with myocardial infarction. We previously indicated that endothelium-dependent relaxations to acetylcholine are completely lacking in the triple NOSs$^{-/-}$ mice and that contractions to phenylephrine are markedly enhanced, suggesting the presence of vascular dysfunction in the triple NOSs$^{-/-}$ mice [11]. Thus, it is likely that acute myocardial infarction in the 2/3NX triple NOSs$^{-/-}$ mice resulted from coronary arteriosclerosis, coronary thrombosis, and coronary vasospasm.

Heart rate variability is considered a noninvasive marker to evaluate autonomic nervous system function. It has been reported that low heart rate variability has prognostic value in patients with myocardial infarction and is associated with a higher risk of death in patients with coronary artery disease [28,29]. Consistent with the findings, significantly lower LF/HF ratio was noted in the 2/3NX triple NOSs$^{-/-}$ mice.

4.2. Clinical implications

Several lines of evidence imply the clinical significance of the 2/3NX triple NOSs$^{-/-}$ model. First, the natural course in which acute myocardial infarction occurs in the triple NOSs$^{-/-}$ mice with partial nephrectomy closely resembles the clinical course in which patients with CKD develop acute myocardial infarction. Second, it has been suggested that the defective NOSs system is present in patients with CKD [30], as evidenced by the facts that in such patients urinary NOx excretion, a marker of systemic NO production derived from all three types of NOSs, are reduced [31], that whole body NO production (assessed by giving an intravenous infusion of [$^{15}N_2$]-arginine and measuring isotopic plasma enrichment of [^{15}N]-citrulline) is decreased [32], and that plasma levels of asymmetric dimethylarginine (ADMA), an endogenous NOS inhibitor, are elevated [33]. Finally, it has been reported that the defective NOSs system also exists in patients with coronary arteriosclerosis and myocardial infarction, as demonstrated by the findings that plasma and/or urinary NOx levels are reduced in such patients [34], that plasma ADMA concentrations are elevated in patients with arteriosclerosis and risk of myocardial infarction [35], and that the NOS gene polymorphisms are associated with arteriosclerosis, risk of myocardial infarction, and low plasma NOx levels in humans [36]. Thus, our acute myocardial infarction model may have clinical implications. However, since pathological conditions of the 2/3NX triple NOSs$^{-/-}$ mice may be different from those of the patients with CKD, results obtained from our model must be interpreted with caution.

4.3. Mechanisms for acute myocardial infarction in the 2/3NX triple NOSs$^{-/-}$ mice

Because significant increases in systolic blood pressure, plasma total cholesterol levels, and fasting blood glucose levels were noted in the 2/3NX triple NOSs$^{-/-}$ mice, a clustering of cardiovascular risk factors seems to be involved in the pathogenesis of their acute myocardial infarction. In agreement with this evidence, it has been shown that patients with CKD have a high prevalence of those cardiovascular risk factors, and that those factors are associated with increased risks of acute myocardial infarction and sudden cardiac death [37].

It has recently been reported that bone marrow-derived mononuclear cells differentiate into VSMC progenitor cells, which circulate in

Fig. 8. Effects of treatment with an AT1 receptor blocker, irbesartan; a calcium channel antagonist, amlodipine; a combination of irbesartan and amlodipine; or an anti-hypertensive agent, hydralazine, on cardiovascular risk factors and SDF-1α-induced recruitment of circulating bone marrow-derived VSMC progenitor cells in the 2/3NX triple NOSs$^{-/-}$ mice. (A) Systolic blood pressure ($n = 10$–12). (B) Plasma total cholesterol levels ($n = 10$–12). (C) Fasting blood glucose levels ($n = 10$–12). (D and E) The number of circulating Sca-1^{+}/c-Kit^{-}/Lin^{-} cells ($n = 7$). (F) Cardiac SDF-1α protein levels ($n = 7$). $^{*}P < 0.05$ vs. none (untreated control).

the blood, accumulate in vascular wall, and contribute to vascular lesion formation [38,39]. It has also been shown that the CXC chemokine SDF-1α is a pivotal chemotactic factor of bone marrow-derived VSMC progenitor cells [40]. In the present study, the number of circulating Sca-1$^+$/c-Kit$^-$/Lin$^-$ cells (interpreted as bone marrow-derived VSMC progenitor cells) [41] and the cardiac SDF-1α protein levels were markedly increased in the 2/3NX triple NOSs$^{-/-}$ mice. Thus, it is possible that SDF-1α-induced recruitment of the circulating bone marrow-derived VSMC progenitor cells was also involved in the occurrence of acute myocardial infarction in the 2/3NX triple NOSs$^{-/-}$ mice.

Renin–angiotensin system activation (as evidenced by increases in plasma angiotensin II levels and cardiac ACE expression levels) and oxidative stress (as indicated by elevation in urinary 8-isoprostane levels) were noted in the 2/3NX triple NOSs$^{-/-}$ mice. Based on these findings, we used the selective and potent AT1 receptor blocker, irbesartan, and the antioxidant calcium channel antagonist, amlodipine, to further examine the involvement of renin–angiotensin system activation and oxidative stress in the pathogenesis of acute myocardial infarction. It has been indicated that amlodipine is a charged molecule, is highly lipophilic, and has a much higher affinity for lipid-laden cellular membranes than do other calcium channel antagonists, exerting a powerful antioxidant activity, independent of its calcium channel antagonistic action [42]. In the present study, the simultaneous treatment with irbesartan and amlodipine potently suppressed renin–angiotensin system activation and oxidative stress, and markedly prevented coronary arteriosclerotic lesion formation and the incidence of myocardial infarction, and improved the prognosis of the 2/3NX triple NOSs$^{-/-}$ mice. Furthermore, the simultaneous irbesartan/amlodipine treatment significantly ameliorated the cardiovascular risk factors, the increased number of circulating Sca-1$^+$/c-Kit$^-$/Lin$^-$ cells, and the enhanced cardiac SDF-1α expression levels in those mice. Therefore, it is conceivable that renin–angiotensin system activation and oxidative stress are involved in the pathogenesis of acute myocardial infarction in the 2/3NX triple NOSs$^{-/-}$ mice. Consistent with these results, it has been reported that renin–angiotensin system activation and oxidative stress are recognized in patients with CKD, and that both factors accelerate arteriosclerotic lesion formation [13].

The treatment with hydralazine exerted an anti-hypertensive action to the same extent as the combined treatment with irbesartan and amlodipine. However, the hydralazine treatment did not show any beneficial effects on the incidence of myocardial infarction, the prognosis, or the pro-arteriosclerotic parameters in the 2/3NX triple NOSs$^{-/-}$ mice. Thus, it is suggested that the beneficial effects of the irbesartan/amlodipine treatment are not caused by changes of blood pressure.

4.4. Clinical perspectives

The mechanism(s) by which CKD is complicated by acute myocardial infarction is not fully understood. Our findings provide novel evidence that the NO/NOSs system plays a pivotal role in the pathogenesis of this reno-cardiac connection. The AT1 receptor blockers and calcium channel antagonists are widely used to treat hypertension in patients with CKD, and the former are also employed to retard the progression of CKD. In the present study, the clinical dosage of irbesartan and amlodipine exhibited cardiovascular and renal protective actions in the 2/3NX triple NOSs$^{-/-}$ mice. These results suggest the therapeutic importance of the AT1 receptor blockers and calcium channel antagonists in preventing complications of acute myocardial infarction in CKD as well as the progression of CKD.

4.5. Conclusions

We have succeeded in developing a novel experimentally useful model of acute myocardial infarction. Renin–angiotensin system activation, oxidative stress, cardiovascular risk factors, and SDF-1α-induced recruitment of circulating bone marrow-derived VSMC progenitor cells appear to be involved in the pathogenesis of acute myocardial infarction in the 2/3NX triple NOSs$^{-/-}$ mice. This model may contribute to the elucidation of the pathogenesis of acute myocardial infarction, and to the research and development of novel therapeutic strategies for preventing this fatal cardiovascular disorder.

Sources of funding

This work was supported in part by a Grant-in-Aid for Scientific Research from the Japan Society for the Promotion of Science (23590305), Special Account Budgets for Education and Research granted by the Japan Ministry of Education, Grants from the Promotion Project of Medical Clustering of Okinawa prefecture and the University of the Ryukyus, and a Grant and Donation from the Sumitomo Dainippon Pharma Co, Japan. These funding sources had no involvement regarding the conduct of the research or preparation of the article.

Conflict of interest

We obtained irbesartan and amlodipine from the Sumitomo Dainippon Pharma Co, Japan, and received a research fund and donation from the company.

Appendix A. Supplementary data

Supplementary data to this article can be found online at http://dx.doi.org/10.1016/j.yjmcc.2014.09.021.

References

[1] White HD, Chew DP. Acute myocardial infarction. Lancet 2008;372:570–84.
[2] Antman EM. ST-segment elevation myocardial infarction: pathology, pathophysiology, and clinical features. In: Libby P, Bonow RO, Mann D, Zipes DP, editors. Braunwald's Heart Disease. 9th ed. Philadelphia: Elsevier Saunders; 2012. p. 1087–110.
[3] Antman EM, Loscaldo J. ST-segment elevation myocardial infarction. In: Longo DL, Fauci AS, Kasper DL, Hauser SL, Jameson JL, Loscalzo J, editors. Harrison's Principles of Internal Medicine. 18th ed. New York: Mc Graw Hill Medical; 2012. p. 2012–35.
[4] Bredt DS, Snyder SH. Nitric oxide: a physiological messenger molecule. Annu Rev Biochem 1994;63:175–95.
[5] Ignarro LJ. Biosynthesis and metabolism of endothelium-derived nitric oxide. Annu Rev Pharmacol Toxicol 1990;30:535–60.
[6] Moncada S, Palmer RMJ, Higgs EA. Nitric oxide: physiology, pathophysiology, and pharmacology. Pharmacol Rev 1991;43:109–42.
[7] Murad F. What are the molecular mechanisms for the antiproliferative effects of nitric oxide and cGMP in vascular smooth muscle? Circulation 1997;95:1101–3.
[8] Shimokawa H. Primary endothelial dysfunction: atherosclerosis. J Mol Cell Cardiol 1999;31:23–37.
[9] Tsutsui M, Shimokawa H, Otsuji Y, Yanagihara N. Pathophysiological relevance of NO signaling in the cardiovascular system: novel insight from mice lacking all NO synthases. Pharmacol Ther 2010;128:499–508.
[10] Morishita T, Tsutsui M, Shimokawa H, Sabanai K, Tasaki H, Suda O, et al. Nephrogenic diabetes insipidus in mice lacking all nitric oxide synthase isoforms. Proc Natl Acad Sci U S A 2005;102:10616–21.
[11] Nakata S, Tsutsui M, Shimokawa H, Suda O, Morishita T, Shibata K, et al. Spontaneous myocardial infarction in mice lacking all nitric oxide synthase isoforms. Circulation 2008;117:2211–23.
[12] Coresh J, Selvin E, Stevens LA, Manzi J, Kusek JW, Eggers P, et al. Prevalence of chronic kidney disease in the United States. JAMA 2007;298:2038–47.
[13] Lopez-Novoa JM, Martinez-Salgado C, Rodriguez-Pena AB, Lopez-Hernandez FJ. Common pathophysiological mechanisms of chronic kidney disease: therapeutic perspectives. Pharmacol Ther 2010;128:61–81.
[14] Ninomiya T, Kiyohara Y, Kubo M, Tanizaki Y, Doi Y, Okubo K, et al. Chronic kidney disease and cardiovascular disease in a general Japanese population: the Hisayama Study. Kidney Int 2005;68:228–36.
[15] Ninomiya T, Kiyohara Y, Tokuda Y, Doi Y, Arima H, Harada A, et al. Impact of kidney disease and blood pressure on the development of cardiovascular disease: an overview from the Japan Arteriosclerosis Longitudinal Study. Circulation 2008;118:2694–701.
[16] Shoji T, Abe T, Matsuo H, Egusa G, Yamasaki Y, Kashihara N, et al. Chronic kidney disease, dyslipidemia, and atherosclerosis. J Atheroscler Thromb 2012;19:299–315.
[17] Miyazaki-Anzai S, Levi M, Kratzer A, Ting TC, Lewis LB, Miyazaki M. Farnesoid X receptor activation prevents the development of vascular calcification in ApoE−/− mice with chronic kidney disease. Circ Res 2010;106:1807–17.

[18] Pelletier CC, Koppe L, Croze ML, Kalbacher E, Vella RE, Guebre-Egziabher F, et al. White adipose tissue overproduces the lipid-mobilizing factor zinc alpha2-glycoprotein in chronic kidney disease. Kidney Int 2013;83:878–86.
[19] Schober A, Knarren S, Lietz M, Lin EA, Weber C. Crucial role of stromal cell-derived factor-1alpha in neointima formation after vascular injury in apolipoprotein E-deficient mice. Circulation 2003;108:2491–7.
[20] Moreno Junior H, Nathan LP, Metze K, Costa SK, Antunes E, Hyslop S, et al. Non-specific inhibitors of nitric oxide synthase cause myocardial necrosis in the rat. Clin Exp Pharmacol Physiol 1997;24:349–52.
[21] Ono Y, Ono H, Matsuoka H, Fujimori T, Frohlich ED. Apoptosis, coronary arterial remodeling, and myocardial infarction after nitric oxide inhibition in SHR. Hypertension 1999;34:609–16.
[22] Verhagen AM, Hohbach J, Joles JA, Braam B, Boer P, Koomans HA, et al. Unchanged cardiac angiotensin II levels accompany losartan-sensitive cardiac injury due to nitric oxide synthase inhibition. Eur J Pharmacol 2000;400:239–47.
[23] Ikeda K, Nara Y, Tagami M, Yamori Y. Nitric oxide deficiency induces myocardial infarction in hypercholesterolaemic stroke-prone spontaneously hypertensive rats. Clin Exp Pharmacol Physiol 1997;24:344–8.
[24] Suda O, Tsutsui M, Morishita T, Tanimoto A, Horiuchi M, Tasaki H, et al. Long-term treatment with N(omega)-nitro-L-arginine methyl ester causes arteriosclerotic coronary lesions in endothelial nitric oxide synthase-deficient mice. Circulation 2002;106:1729–35.
[25] Braun A, Trigatti BL, Post MJ, Sato K, Simons M, Edelberg JM, et al. Loss of SR-BI expression leads to the early onset of occlusive atherosclerotic coronary artery disease, spontaneous myocardial infarctions, severe cardiac dysfunction, and premature death in apolipoprotein E-deficient mice. Circ Res 2002;90:270–6.
[26] Zhang S, Picard MH, Vasile E, Zhu Y, Raffai RL, Weisgraber KH, et al. Diet-induced occlusive coronary atherosclerosis, myocardial infarction, cardiac dysfunction, and premature death in scavenger receptor class B type I-deficient, hypomorphic apolipoprotein ER61 mice. Circulation 2005;111:3457–64.
[27] Nakagawa-Toyama Y, Zhang S, Krieger M. Dietary manipulation and social isolation alter disease progression in a murine model of coronary heart disease. PLoS One 2012;7:e47965.
[28] Taddei S, Virdis A, Ghiadoni L, Magagna A, Favilla S, Pompella A, et al. Restoration of nitric oxide availability after calcium antagonist treatment in essential hypertension. Hypertension 2001;37:943–8.
[29] Tsuji H, Venditti Jr FJ, Manders ES, Evans JC, Larson MG, Feldman CL, et al. Reduced heart rate variability and mortality risk in an elderly cohort. The Framingham Heart Study. Circulation 1994;90:878–83.
[30] Baylis C. Nitric oxide deficiency in chronic kidney disease. Am J Physiol Renal Physiol 2008;294:F1–9.
[31] Schmidt RJ, Baylis C. Total nitric oxide production is low in patients with chronic renal disease. Kidney Int 2000;58:1261–6.
[32] Wever R, Boer P, Hijmering M, Stroes E, Verhaar M, Kastelein J, et al. Nitric oxide production is reduced in patients with chronic renal failure. Arterioscler Thromb Vasc Biol 1999;19:1168–72.
[33] Lu TM, Chung MY, Lin CC, Hsu CP, Lin SJ. Asymmetric dimethylarginine and clinical outcomes in chronic kidney disease. Clin J Am Soc Nephrol 2011;6:1566–72.
[34] Piatti P, Di Mario C, Monti LD, Fragasso G, Sgura F, Caumo A, et al. Association of insulin resistance, hyperleptinemia, and impaired nitric oxide release with in-stent restenosis in patients undergoing coronary stenting. Circulation 2003;108:2074–81.
[35] Cooke JP. ADMA: its role in vascular disease. Vasc Med 2005;10(Suppl. 1):S11–7.
[36] Cook S. Coronary artery disease, nitric oxide and oxidative stress: the "Yin-Yang" effect, a Chinese concept for a worldwide pandemic. Swiss Med Wkly 2006;136:103–13.
[37] Shamseddin MK, Parfrey PS. Sudden cardiac death in chronic kidney disease: epidemiology and prevention. Nat Rev Nephrol 2011;7:145–54.
[38] Sata M, Saiura A, Kunisato A, Tojo A, Okada S, Tokuhisa T, et al. Hematopoietic stem cells differentiate into vascular cells that participate in the pathogenesis of atherosclerosis. Nat Med 2002;8:403–9.
[39] Shimizu K, Sugiyama S, Aikawa M, Fukumoto Y, Rabkin E, Libby P, et al. Host bone-marrow cells are a source of donor intimal smooth- muscle-like cells in murine aortic transplant arteriopathy. Nat Med 2001;7:738–41.
[40] Ceradini DJ, Kulkarni AR, Callaghan MJ, Tepper OM, Bastidas N, Kleinman ME, et al. Progenitor cell trafficking is regulated by hypoxic gradients through HIF-1 induction of SDF-1. Nat Med 2004;10:858–64.
[41] Zhang LN, Wilson DW, da Cunha V, Sullivan ME, Vergona R, Rutledge JC, et al. Endothelial NO synthase deficiency promotes smooth muscle progenitor cells in association with upregulation of stromal cell-derived factor-1alpha in a mouse model of carotid artery ligation. Arterioscler Thromb Vasc Biol 2006;26:765–72.
[42] Mason RP, Walter MF, Trumbore MW, Olmstead Jr EG, Mason PE. Membrane antioxidant effects of the charged dihydropyridine calcium antagonist amlodipine. J Mol Cell Cardiol 1999;31:275–81.

Neurosteroids Allopregnanolone Sulfate and Pregnanolone Sulfate Have Diverse Effect on the α Subunit of the Neuronal Voltage-gated Sodium Channels $Na_v1.2$, $Na_v1.6$, $Na_v1.7$, and $Na_v1.8$ Expressed in *Xenopus* Oocytes

Takafumi Horishita, M.D., Ph.D., Nobuyuki Yanagihara, Ph.D., Susumu Ueno, M.D., Ph.D., Yuka Sudo, Ph.D., Yasuhito Uezono, M.D., Ph.D., Dan Okura, M.D., Tomoko Minami, M.D., Takashi Kawasaki, M.D., Ph.D., Takeyoshi Sata, M.D., Ph.D.

ABSTRACT

Background: The neurosteroids allopregnanolone and pregnanolone are potent positive modulators of γ-aminobutyric acid type A receptors. Antinociceptive effects of allopregnanolone have attracted much attention because recent reports have indicated the potential of allopregnanolone as a therapeutic agent for refractory pain. However, the analgesic mechanisms of allopregnanolone are still unclear. Voltage-gated sodium channels (Na_v) are thought to play important roles in inflammatory and neuropathic pain, but there have been few investigations on the effects of allopregnanolone on sodium channels.

Methods: Using voltage-clamp techniques, the effects of allopregnanolone sulfate (APAS) and pregnanolone sulfate (PAS) on sodium current were examined in *Xenopus* oocytes expressing $Na_v1.2$, $Na_v1.6$, $Na_v1.7$, and $Na_v1.8$ α subunits.

Results: APAS suppressed sodium currents of $Na_v1.2$, $Na_v1.6$, and $Na_v1.7$ at a holding potential causing half-maximal current in a concentration-dependent manner, whereas it markedly enhanced sodium current of $Na_v1.8$ at a holding potential causing maximal current. Half-maximal inhibitory concentration values for $Na_v1.2$, $Na_v1.6$, and $Na_v1.7$ were 12 ± 4 (n = 6), 41 ± 2 (n = 7), and 131 ± 15 (n = 5) μmol/l (mean ± SEM), respectively. The effects of PAS were lower than those of APAS. From gating analysis, two compounds increased inactivation of all α subunits, while they showed different actions on activation of each α subunit. Moreover, two compounds showed a use-dependent block on $Na_v1.2$, $Na_v1.6$, and $Na_v1.7$.

Conclusion: APAS and PAS have diverse effects on sodium currents in oocytes expressing four α subunits. APAS inhibited the sodium currents of $Na_v1.2$ most strongly. **(ANESTHESIOLOGY 2014; 121:620-31)**

NEUROSTEROIDS are neuroactive steroids synthesized from cholesterol in both central and peripheral nervous systems, and they accumulate in the nervous system.[1] They rapidly alter neuronal excitability by mediating actions through ion-gated neurotransmitter receptors, but not through classic steroid hormone nuclear receptors.[2] Many of them are converted to sulfated metabolites by hydroxysteroid sulfotransferases, and neurosteroid sulfates are also known to regulate physiological processes. They are thought to be potentially therapeutic because of their many pharmacological properties.[3,4]

Two 3α-hydroxylated metabolites of progesterone, allopregnanolone (3α-hydroxy-5α-pregnane-20-one) and pregnanolone (3α-hydroxy-5β-pregnane-20-one), are known to be positive modulators at γ-aminobutyric acid type A ($GABA_A$) receptors with high potency.[5] These neurosteroids have been shown to have greater anesthetic potencies than those of other intravenous anesthetics that are clinically used, and not to cause acute tolerance that are observed in other

What We Already Know about This Topic

- Sodium channels are important targets for analgesic actions in the spinal cord, but their role in neurosteroid analgesia is unclear
- The effects of two sulfated neurosteroids with analgesic and anesthetic properties were tested on heterologously expressed rat voltage-gated sodium channel function

What This Article Tells Us That Is New

- The neurosteroids tested produced voltage and use-dependent block of all the subtypes tested, with more potent effects on $Na_v1.2$
- Inhibition of $Na_v1.2$ in the spinal cord by allopregnanolone is a plausible mechanism for its analgesic effects if confirmed in neuronal preparations and pain models

Submitted for publication October 25, 2013. Accepted for publication April 9, 2014. From the Department of Anesthesiology (T.H., D.O., T.M., T.K., T.S.) and Department of Pharmacology (N.Y.), School of Medicine, University of Occupational and Environmental Health, Kitakyushu, Japan; Department of Occupational Toxicology, Institute of Industrial Ecological Sciences, University of Occupational and Environmental Health, Kitakyushu, Japan (S.U.); Department of Molecular Pathology and Metabolic Disease, Faculty of Pharmaceutical Sciences, Tokyo University of Science, Chiba, Japan (Y.S.); and Cancer Pathophysiology Division, National Cancer Center Research Institute, Tokyo, Japan (Y.U.).

 Anesthesiology 2014; 121:620-31

anesthetics, suggesting usefulness of these neurosteroids as general anesthetics.[6,7] On the contrary, allopregnanolone was shown to have the most potent analgesic effects among all neurosteroids in pain models.[8] Recent studies demonstrated its analgesic effects in neuropathic pain models. Allopregnanolone alleviates thermal and mechanical hyperalgesia by ligation of the sciatic nerve in rats,[9] produces analgesic effects on formalin-induced pain in rats,[10] and prevents anticancer drug oxaliplatin-induced cold and mechanical allodynia and hyperalgesia.[11] In addition, it was suggested that stimulation of allopregnanolone synthesis might be involved in the antinociceptive effects of several analgesic drugs in neuropathic pain models.[12–14] Its effect on $GABA_A$ receptors may be important for its antinociceptive properties because GABA is involved in pain pathways in the nervous systems, and drugs targeting subtypes of GABA receptors have analgesic effects in chronic pain.[15] However, these two neurosteroids, allopregnanolone and pregnanolone, also act on other ion channels in pain signaling pathways, including T-type calcium channels[16] and *N*-methyl-D-aspartate receptors.[17]

Voltage-gated sodium channels (Na_v) have an important role in action potential initiation and propagation in excitable nerve and muscle cells. Nine α subunits ($Na_v1.1$ to $Na_v1.9$) and four auxiliary β subunits have been identified in mammals.[18,19] Each pore-forming α subunit has a different pattern of development and localization and has distinct physiological and pathophysiological roles. Sodium channel α subunits expressed in the dorsal root ganglion are considered possible targets for analgesics for inflammatory and neuropathic pain.[20–22] However, there has been little investigation on the effects of allopregnanolone on sodium channel function. It is important to examine these effects because they may be useful in clarifying the mechanisms of the analgesic effects of allopregnanolone and developing natural and safe neurosteroid-based analgesics for refractory pain. In addition, our recent report demonstrated the importance of neurosteroid sulfonation for regulation of ion channels because of more potent effects of sulfated steroid than those of nonsulfated steroids.[23] Here, we investigate the effects of two sulfated neurosteroids, allopregnanolone sulfate (APAS) and pregnanolone sulfate (PAS) (fig. 1), on several sodium channel α subunits, including $Na_v1.2$, which is expressed in the central nervous system; $Na_v1.6$, which is expressed in the central nervous system and dorsal root ganglion neurons; and $Na_v1.7$ and $Na_v1.8$, which are expressed in dorsal root ganglion neurons.

Materials and Methods

This study was approved by the Animal Research Committee of the University of Occupational and Environmental Health, Kitakyushu, Japan.

Drugs

Allopregnanolone sulfate and PAS were purchased from Steraloids, Inc. (Newport, RI).

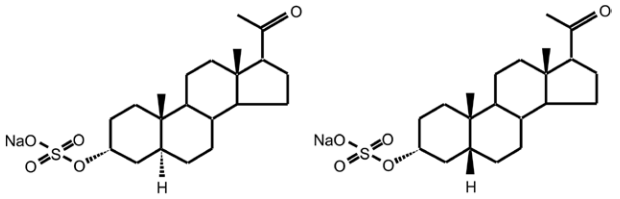

Fig. 1. Structures of allopregnanolone sulfate (APAS) and pregnanolone sulfate (PAS).

Plasmids

Rat $Na_v1.2$ α subunit complementary DNA (cDNA) was a gift from Dr. William A. Catterall, Ph.D. (Professor, Department of Pharmacology, University of Washington, Seattle, Washington). Rat $Na_v1.6$ α subunit cDNA was a gift from Dr. Alan L. Goldin, M.D., Ph.D. (Professor, Department of Anatomy and Neurobiology, University of California, Irvine, California). Rat $Na_v1.7$ α subunit cDNA was a gift from Gail Mandel, Ph.D. (Professor, Department of Biochemistry and Molecular Biology, Oregon Health and Science University, Portland, Oregon). Rat $Na_v1.8$ α subunit cDNA was a gift from Dr. Armen N. Akopian, Ph.D. (Assistant Professor, University of Texas Health Science Center, San Antonio, Texas), and human β_1 subunit cDNA was a gift from Dr. Alfred L. George, Jr., M.D. (Professor, Department of Pharmacology, Vanderbilt University, Nashville, Tennessee). The percentages of homology between rat and human protein of $Na_v1.2$, $Na_v1.6$, $Na_v1.7$, and $Na_v1.8$ are 98, 99, 93, and 83%, respectively, suggesting the possible limitations imposed by using rat α subunit for only $Na_v1.8$ to make conclusions in humans.

Complementary RNA (cRNA) Preparation and Oocyte Injection

After linearization of cDNA with *Cla*I ($Na_v1.2$ α subunit), *Not*I ($Na_v1.6$, 1.7 α subunits), *Xba*I ($Na_v1.8$ α subunit), and *EcoR*I (β_1 subunit), cRNAs were transcribed using SP6 (Na_v 1.8 α, β_1 subunits) or T7 ($Na_v1.2$, 1.6, and 1.7 α subunits) RNA polymerase from the mMESSAGE mMACHINE kit (Ambion, Austin, TX). Adult female *Xenopus laevis* frogs were obtained from Kyudo Co., Ltd. (Saga, Japan). *X. laevis* oocytes and cRNA microinjection were prepared as described previously.[24] Na_v α subunit cRNAs were coinjected with β_1 subunit cRNA at a ratio of 1:10 (total volume was 20 to 40 ng/50 nl) into *Xenopus* oocytes (all α subunits were coinjected with the β_1 subunit) that were randomly assigned to four α subunit groups for injection. Injected oocytes were incubated at 19°C in incubation medium, and 2 to 6 days after injection, the cells were used for electrophysiological recordings.

Electrophysiological Recordings

All electrical recordings were performed at room temperature (23°C). Oocytes were placed in a 100-μl recording chamber

and perfused at 2 ml/min with Frog Ringer's solution containing 115 mmol/l NaCl, 2.5 mmol/l KCl, 10 mmol/l HEPES, 1.8 mmol/l $CaCl_2$, pH 7.2, using a peristaltic pump (World Precision Instruments Inc., Sarasota, FL). Recording electrodes were prepared, and the whole-cell voltage clamp and recordings were achieved as described previously.[24] Transients and leak currents were subtracted using the P/N procedure, in which N subsweeps each 1/Nth of the amplitude of the main stimulus waveform (P) are applied. APAS and PAS stocks were prepared in dimethylsulfoxide and diluted in Frog Ringer's solution to a final dimethylsulfoxide concentration not exceeding 0.05%. APAS and PAS were perfused for 3 min to reach equilibrium. All recordings were performed by the experimenters who were blind to the type of compound.

The voltage dependence of activation was determined using 50-ms depolarizing pulses from a holding potential causing maximal current (V_{max}) (–90 mV for $Na_v1.2$ and $Na_v1.6$, –100 mV for $Na_v1.7$ and $Na_v1.8$) and from a holding potential causing half-maximal current ($V_{1/2}$) (from approximately –40 mV to –70 mV) to 60 mV in 10-mV increments. V_{max} and $V_{1/2}$ holding potentials induce resting and inactivated states of sodium channels. Because the effects of many analgesics in the inactivated state are known to be important for analgesic action,[25] we used these two different holding potentials to compare the effects of compounds in the resting and inactivated states. Normalized activation curves were fitted to the Boltzmann equation as described previously[24]: briefly, $G/G_{max} = 1/(1 + \exp(V_{1/2} - V)/k)$, where G is the voltage-dependent sodium conductance, G_{max} is the maximal sodium conductance, G/G_{max} is the normalized fractional conductance, $V_{1/2}$ is the potential at which activation is half maximal, and k is the slope factor. To measure steady-state inactivation, currents were elicited by a 50-ms test pulse to –20 mV for $Na_v1.2$ and $Na_v1.6$, –10 mV for $Na_v1.7$, and +10 mV for $Na_v1.8$ after 200 ms (500 ms for only $Na_v1.8$) prepulses ranging from –140 to 0 mV in 10-mV increments from a holding potential of V_{max}. Steady-state inactivation curves were fitted to the Boltzmann equation: $I/I_{max} = 1/(1 + \exp(V_{1/2} - V)/k)$, where I_{max} is the maximal sodium current, I/I_{max} is the normalized current, $V_{1/2}$ is the voltage of half-maximal inactivation, and k is the slope factor. To investigate a use-dependent sodium channel block, currents were elicited at 10 Hz by a 20-ms depolarizing pulse of –20 mV for $Na_v1.2$ and $Na_v1.6$, –10 mV for $Na_v1.7$, and +10 mV for $Na_v1.8$ from a $V_{1/2}$ holding potential in both the absence and presence of 100 μmol/l APAS and PAS. Peak currents were measured and normalized to the first pulse and plotted against the pulse number. Data were fitted to the monoexponential equation $I_{Na} = \exp(-\tau_{use} \cdot n) + C$, where n is pulse number, C is the plateau I_{Na}, and τ_{use} is the time constant of use-dependent decay.

Statistical Analysis

The GraphPad Prism software (GraphPad Software, Inc., San Diego, CA) was used to perform the statistical analysis, and a statistical power analysis was performed using G*Power software. All values are presented as means ± SEM. The n values refer to the number of oocytes examined. Each experiment was performed with oocytes taken from at least two frogs. Data were statistically evaluated by paired t test (two-tailed). We assessed the inhibitory effects at different APAS concentrations in the concentration–response curve, using one-way ANOVA followed by Dunnet *post hoc* test for multiple comparisons. Hill slope, half-maximal inhibitory concentration (IC_{50}), and half-maximal effective concentration

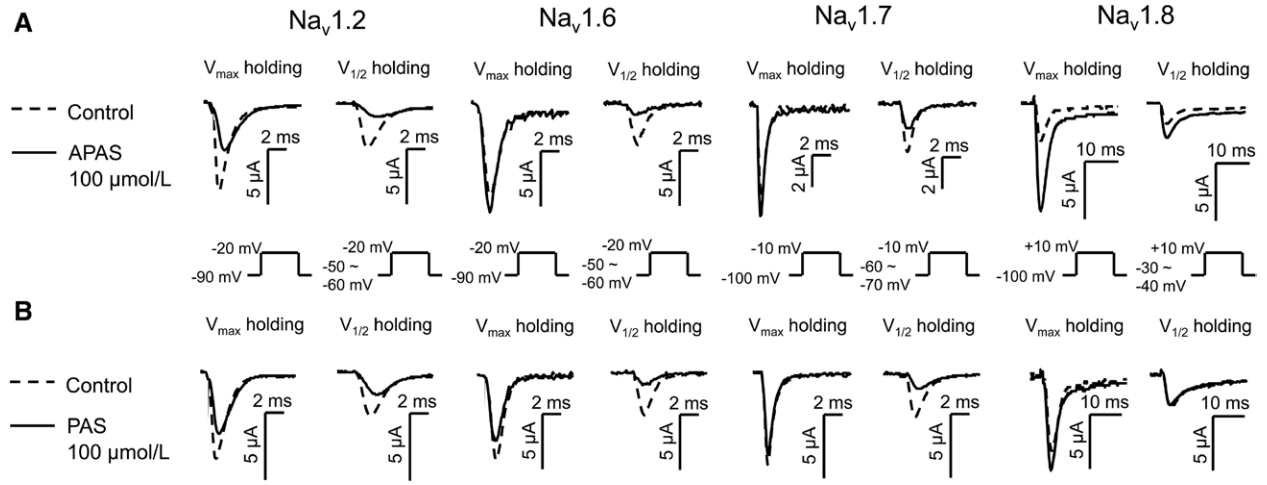

Fig. 2. Effects of allopregnanolone sulfate (APAS) (*A*) and pregnanolone sulfate (PAS) (*B*) on peak sodium inward currents in *Xenopus* oocytes expressing $Na_v1.2$, $Na_v1.6$, $Na_v1.7$, or $Na_v1.8$ α subunits with β_1 subunits at two holding potentials. Representative traces are shown. Sodium currents were evoked by 50-ms depolarizing pulses to –20 mV for $Na_v1.2$ and $Na_v1.6$, –10 mV for $Na_v1.7$, and +10 mV for $Na_v1.8$ from V_{max} or $V_{1/2}$ in both the absence and presence of 100 μmol/l of the compounds. Na_v = voltage-gated sodium channel; V_{max} holding = holding potential causing maximal current; $V_{1/2}$ holding = holding potential causing half-maximal current.

(EC_{50}) values were also calculated. *P* value less than 0.05 was considered to indicate a significant difference.

Results

Effects of APAS and PAS on Peak Na^+ Inward Currents Elicited from Two Different Holding Potentials

Currents were elicited using a 50-ms depolarizing pulse to −20 mV for $Na_v1.2$ and $Na_v1.6$, −10 mV for $Na_v1.7$, and +10 mV for $Na_v1.8$ applied every 10 s from a V_{max} or $V_{1/2}$ holding potential in both the absence and presence of 100 μmol/l APAS and PAS (fig. 2). The amplitude of expressed sodium currents was typically 2 to 15 μA, and oocytes that showed a maximal current greater than 20 μA were not included in the data collection in all the following experiments. APAS had dual effects on sodium currents depending on the holding potential and α subunit (figs. 2 and 3). At $V_{1/2}$, APAS reduced the peak I_{Na} (sodium current) induced by $Na_v1.2$, $Na_v1.6$, and $Na_v1.7$ by 79 ± 1%, 71 ± 2%, and 49 ± 3%, respectively. At V_{max}, APAS also reduced I_{Na} induced by $Na_v1.2$ by 60 ± 4%, whereas it enhanced I_{Na} induced by $Na_v1.6$ and $Na_v1.7$ by 15 ± 6% and 14 ± 1%, respectively, although these effects were small. In contrast, APAS greatly enhanced I_{Na} induced by $Na_v1.8$ at both $V_{1/2}$ and V_{max} by 112 ± 34% and 202 ± 14%, respectively (fig. 3A). PAS reduced I_{Na} induced by $Na_v1.2$, $Na_v1.6$, and $Na_v1.7$ at $V_{1/2}$ by 54 ± 4%, 71 ± 1%, and 48 ± 2%, respectively. Effects of PAS on I_{Na} at V_{max} were smaller than those at $V_{1/2}$, and the magnitudes of inhibitory effects on $Na_v1.2$, $Na_v1.6$, and $Na_v1.7$ were 31 ± 5%, 10 ± 1%, and 6 ± 1%, respectively. While PAS enhanced I_{Na} induced by $Na_v1.8$ at V_{max} by 39 ± 6%, it did not affect I_{Na} induced by $Na_v1.8$ at $V_{1/2}$ (fig. 3B). In summary, PAS inhibited I_{Na} induced by $Na_v1.2$, $Na_v1.6$, and $Na_v1.7$ at both $V_{1/2}$ and V_{max} holding potentials. APAS had inverse effects on $Na_v1.6$ and $Na_v1.7$ according to the different holding potentials, whereas it suppressed I_{Na} induced by $Na_v1.2$ at both $V_{1/2}$ and V_{max}. Moreover, APAS markedly enhanced I_{Na} induced by $Na_v1.8$ at both $V_{1/2}$ and V_{max}.

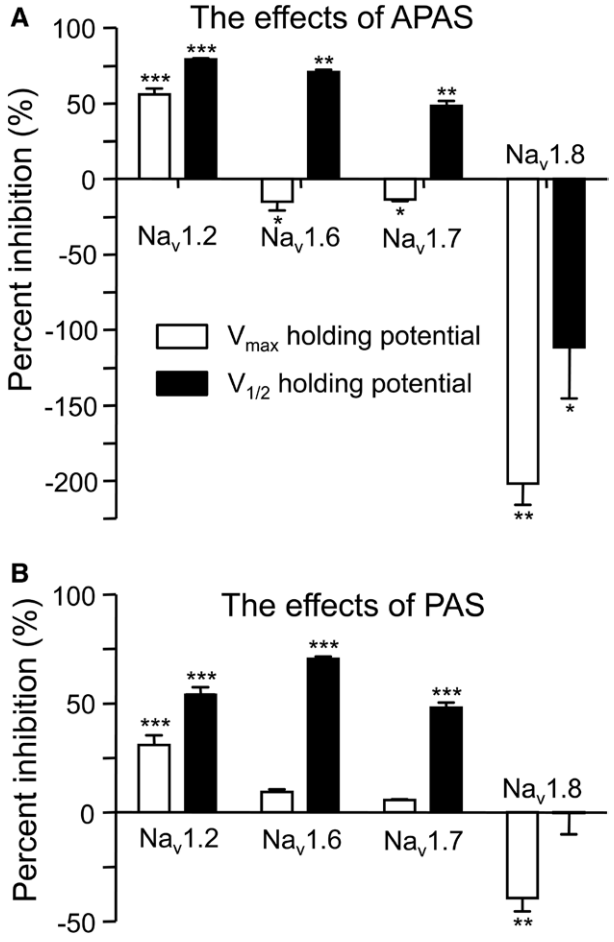

Fig. 3. Percentage inhibition of sodium currents of allopregnanolone sulfate (APAS) (n = 6) (*A*) and pregnanolone sulfate (PAS) (n = 5) (*B*) were calculated. *Open columns* represent the effect at V_{max} holding potential, and *closed columns* indicate the effect at $V_{1/2}$. Data are presented as means ± SEM. **P* < 0.05, ***P* < 0.01, and ****P* < 0.001 compared with the control, based on paired *t* test (two-tailed). Na_v = voltage-gated sodium channel; V_{max} holding potential = holding potential causing maximal current; $V_{1/2}$ holding potential = holding potential causing half-maximal current.

Next, we examined the concentration–response relationship for suppression of the peak I_{Na} induced through $Na_v1.2$, $Na_v1.6$, and $Na_v1.7$ by APAS and PAS at $V_{1/2}$ holding potential because suppression by both neurosteroids of these α subunits at $V_{1/2}$ was more potent than that at V_{max} (fig. 4, A and B). In addition, we investigated the concentration–response relationship for potentiation of the peak I_{Na} of $Na_v1.8$ by APAS and PAS at V_{max}, because both neurosteroids showed potent enhancement of I_{Na} at V_{max} compared with that at $V_{1/2}$ (fig. 4C). IC_{50} values, EC_{50} values, and Hill slopes calculated from nonlinear regression analyses of the dose–response curves are shown in table 1. From these analyses, the effect of APAS on $Na_v1.2$ was the most potent among the two neurosteroids and four α subunits.

Effects of APAS and PAS on Activation of Sodium Currents

We examined the effects of APAS and PAS on four α subunits in sodium current activation. Voltage dependence of activation was determined using 50-ms depolarizing pulses from a holding potential of V_{max} to 50 mV in 10-mV increments or from a holding potential of $V_{1/2}$ to 60 mV in 10-mV increments for $Na_v1.2$, $Na_v1.6$, $Na_v1.7$, and $Na_v1.8$ in both the absence and presence of 100 μmol/l APAS and PAS (fig. 5). Activation curves were derived from the I–V curves (see Electrophysiological Recordings under Materials and Methods). At V_{max}, APAS greatly reduced the peak I_{Na} induced by $Na_v1.2$, whereas it greatly enhanced the peak I_{Na} induced by $Na_v1.8$ in the depolarizing region where channel opening begins. It also enhanced the peak I_{Na} induced by $Na_v1.6$ and $Na_v1.7$, similar to its effects on $Na_v1.8$, although both effects were small. At $V_{1/2}$, APAS greatly suppressed the peak I_{Na} induced by $Na_v1.2$, $Na_v1.6$, and $Na_v1.7$,

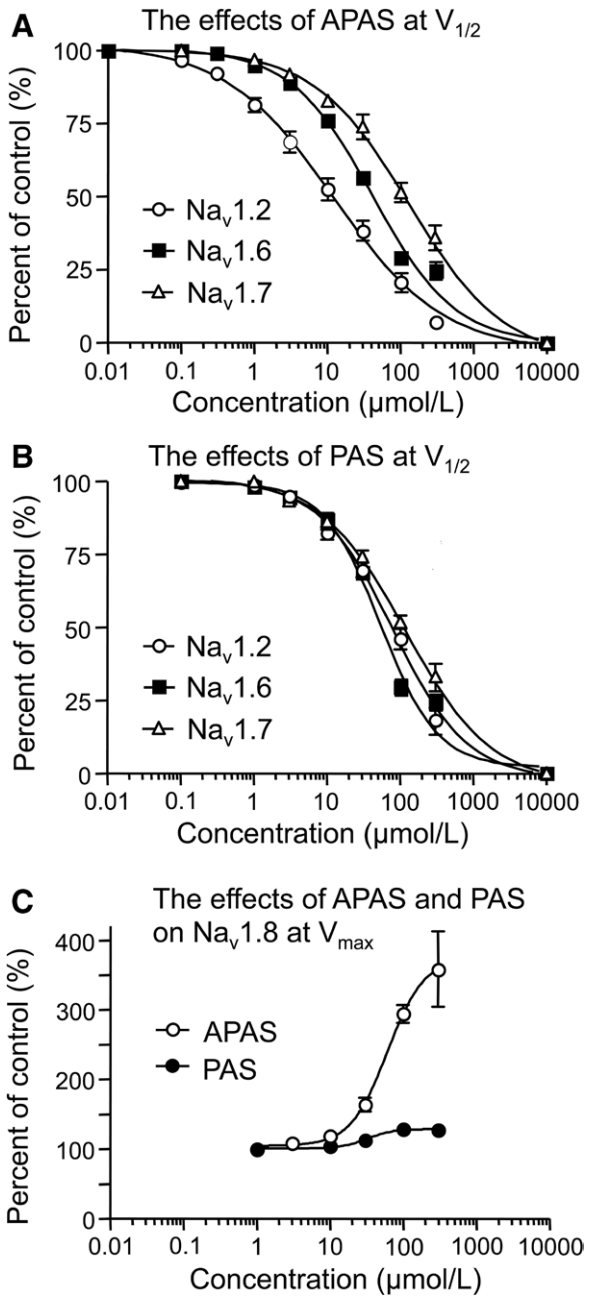

Fig. 4. Concentration–response curves for two-compound suppression of sodium currents elicited by 50-ms depolarizing pulses to –20 mV for $Na_v1.2$ (n = 6) and $Na_v1.6$ (n = 7) and –10 mV for $Na_v1.7$ (n = 5) from $V_{1/2}$ holding potential (*A* and *B*) and those for two-compound potentiation of sodium currents elicited by 50-ms depolarizing pulses to +10 mV for $Na_v1.8$ (n = 5) from V_{max} (*C*). The peak current amplitude in the presence of two compounds was normalized to that of the control, and the effects are expressed as percentages of the control. Hill slopes, IC_{50} values, and EC_{50} values are shown in table 1. Data are presented as means ± SEM. Data were fitted to the Hill slope equation to give the Hill slopes, IC_{50} values, and EC_{50} values. Hill slopes, IC_{50} values, and EC_{50} values were calculated using GraphPad Prism (GraphPad Software, Inc., San Diego, CA). APAS = allopregnanolone sulfate; Na_v = voltage-gated sodium channel; PAS = pregnanolone sulfate; V_{max} = holding potential causing maximal current; $V_{1/2}$ = holding potential causing half-maximal current.

but it enhanced the peak I_{Na} induced by $Na_v1.8$, similar to its effects on $Na_v1.8$ at V_{max}. PAS reduced I_{Na} induced by $Na_v1.2$, $Na_v1.6$, and $Na_v1.7$ at both $V_{1/2}$ and V_{max}, whereas it enhanced I_{Na} induced by $Na_v1.8$ in the depolarizing region at V_{max}, but had no effect at $V_{1/2}$.

At V_{max} holding potential, APAS significantly shifted the midpoint of the steady-state activation ($V_{1/2}$) in a depolarizing direction for $Na_v1.2$, but it significantly shifted $V_{1/2}$ in a hyperpolarizing direction for $Na_v1.6$, $Na_v1.7$, and $Na_v1.8$. At $V_{1/2}$, APAS also shifted $V_{1/2}$ in a similar direction as the shift at V_{max}, although the shift was small and not significant, except for $Na_v1.8$. The shifts of $V_{1/2}$ by PAS were smaller than those by APAS. PAS significantly shifted $V_{1/2}$ in a depolarizing direction for $Na_v1.2$ and $Na_v1.6$ at $V_{1/2}$, but it had no or slight effects on all α subunits at V_{max}, and on $Na_v1.7$ and $Na_v1.8$ at $V_{1/2}$ (fig. 6 and tables 2 and 3).

Effects of APAS and PAS on Inactivation of Sodium Currents

We also investigated the effects of APAS and PAS on steady-state inactivation. Currents were elicited by a 50-ms test pulse to –20 mV for $Na_v1.2$ and $Na_v1.6$, –10 mV for $Na_v1.7$, and +10 mV for $Na_v1.8$ after 200 ms (500 ms for only $Na_v1.8$) prepulses ranging from –140 mV to 0 mV in 10-mV increments from V_{max} holding potential. Steady-state inactivation curves were fitted to the Boltzmann equation (see Electrophysiological Recordings under Materials and Methods). APAS and PAS significantly shifted the midpoint of steady-state inactivation ($V_{1/2}$) in the hyperpolarizing direction for all α subunits; APAS shifted by 8.0, 8.9, 6.7, and 8.9 mV and PAS shifted by 4.5, 8.0, 6.6, and 10.2 mV for $Na_v1.2$, $Na_v1.6$, $Na_v1.7$, and $Na_v1.8$, respectively (fig. 7 and tables 2 and 3). The effects of APAS and PAS in the hyperpolarizing range were consistent with the effects of these two neurosteroids on the peak I_{Na} at V_{max} and their effects on the I–V curves in the hyperpolarizing range at V_{max}.

Use-dependent Block of Sodium Currents by APAS and PAS

The use-dependent block of sodium currents by APAS and PAS was also investigated. Currents were elicited at 10 Hz by a 20-ms depolarizing pulse of –20 mV for $Na_v1.2$ and $Na_v1.6$ and –10 mV for $Na_v1.7$ from a $V_{1/2}$ holding potential in both the absence and presence of 100 μmol/l APAS and PAS. Peak currents were measured and normalized to the first pulse and plotted against the pulse number (fig. 8, A–D). Data were fitted by the monoexponential equation (see Electrophysiological Recordings under Materials and Methods). APAS significantly reduced the plateau I_{Na} amplitude of $Na_v1.2$, $Na_v1.6$, and $Na_v1.7$ from 0.80 ± 0.03 to 0.57 ± 0.03, 0.89 ± 0.01 to 0.49 ± 0.07, and 0.89 ± 0.02 to 0.62 ± 0.06, respectively (fig. 8E). PAS also reduced the plateau I_{Na} amplitudes of $Na_v1.2$, $Na_v1.6$, and $Na_v1.7$ from 0.81 ± 0.2 to 0.70 ± 0.03, 0.94 ± 0.01 to 0.73 ± 0.02, and 0.91 ± 0.02 to 0.75 ± 0.01, respectively, and the reductions

Table 1. Fitted Parameters for Effects of APAS and PAS

	APAS			PAS		
	IC_{50}	EC_{50}	Hill Slope	IC_{50}	EC_{50}	Hill Slope
$Na_v1.2$	12.2 ± 3.5		0.58 ± 0.07	78.4 ± 9.8		0.86 ± 0.03
$Na_v1.6$	40.6 ± 1.9		0.77 ± 0.03	53.8 ± 3.2		1.12 ± 0.03
$Na_v1.7$	130.7 ± 14.7		0.67 ± 0.06	117.8 ± 19.0		0.74 ± 0.04
$Na_v1.8$		61.3 ± 8.5	1.72 ± 0.10		32.7 ± 3.4	2.45 ± 0.47

IC_{50} values, EC_{50} values, and Hill slopes calculated from nonlinear regression analyses of the dose–response curves shown in figure 4. Data are given as mean ± SEM; n = 6 ($Na_v1.2$), 7 ($Na_v1.6$), 5 ($Na_v1.7$), and 5 ($Na_v1.8$).

APAS = allopregnanolone sulfate; EC_{50} = half-maximal effective concentration; IC_{50} = half-maximal inhibitory concentration; Na_v = voltage-gated sodium channel; PAS = pregnanolone sulfate.

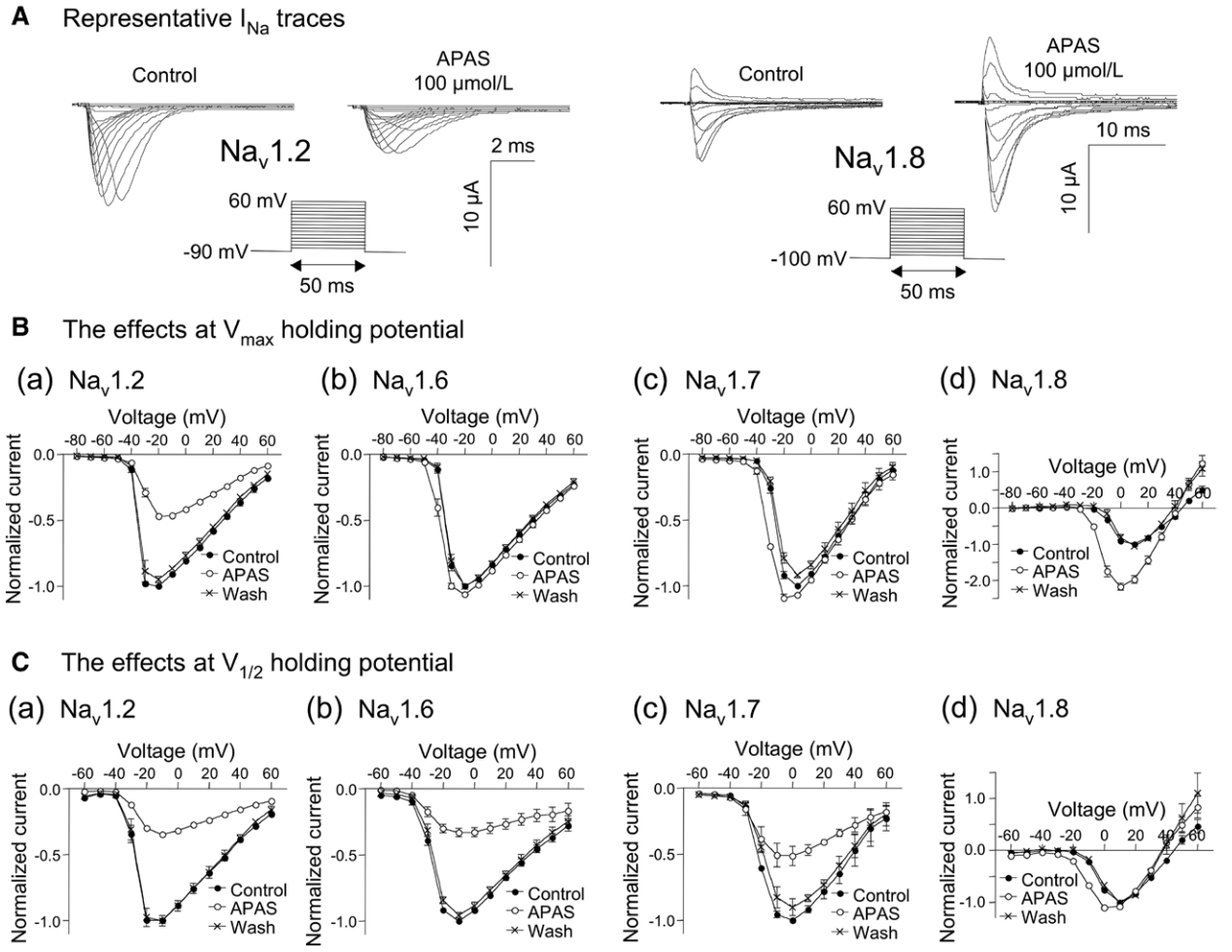

Fig. 5. Effects of allopregnanolone sulfate (APAS) on I–V curves of sodium currents in oocytes expressing $Na_v1.2$ (*a*) (n = 5), $Na_v1.6$ (*b*) (n = 7), $Na_v1.7$ (*c*) (n = 5), or $Na_v1.8$ (*d*) (n = 6) α subunits with β_1 subunits. Currents were elicited using 50-ms depolarizing steps between –80 and 60 mV in 10-mV increments from a V_{max} holding potential and elicited using 50-ms depolarizing steps between –60 and 60 mV in 10-mV increments from a $V_{1/2}$ holding potential. (*A*) Representative I_{Na} traces from oocytes expressing $Na_v1.2$ (*left*) and $Na_v1.8$ (*right*) with the β_1 subunit in both the absence and presence of 100 μmol/l of APAS at V_{max} holding potential are shown. The effects of APAS on normalized I–V curves elicited from V_{max} (*B*) and $V_{1/2}$ holding potentials (*C*) are shown (*closed circles*, control; *open circles*, neurosteroids; *cross*, washout). Peak currents were normalized to the maximal currents observed from –20 to +10 mV. Data are presented as means ± SEM. Na_v = voltage-gated sodium channel; V_{max} holding potential = holding potential causing maximal current; $V_{1/2}$ holding potential = holding potential causing half-maximal current; Wash = washout.

were significant except for $Na_v1.2$ (fig. 8F). These results demonstrated a use-dependent block of APAS and PAS on sodium channels, and the block by APAS was more potent than that by PAS.

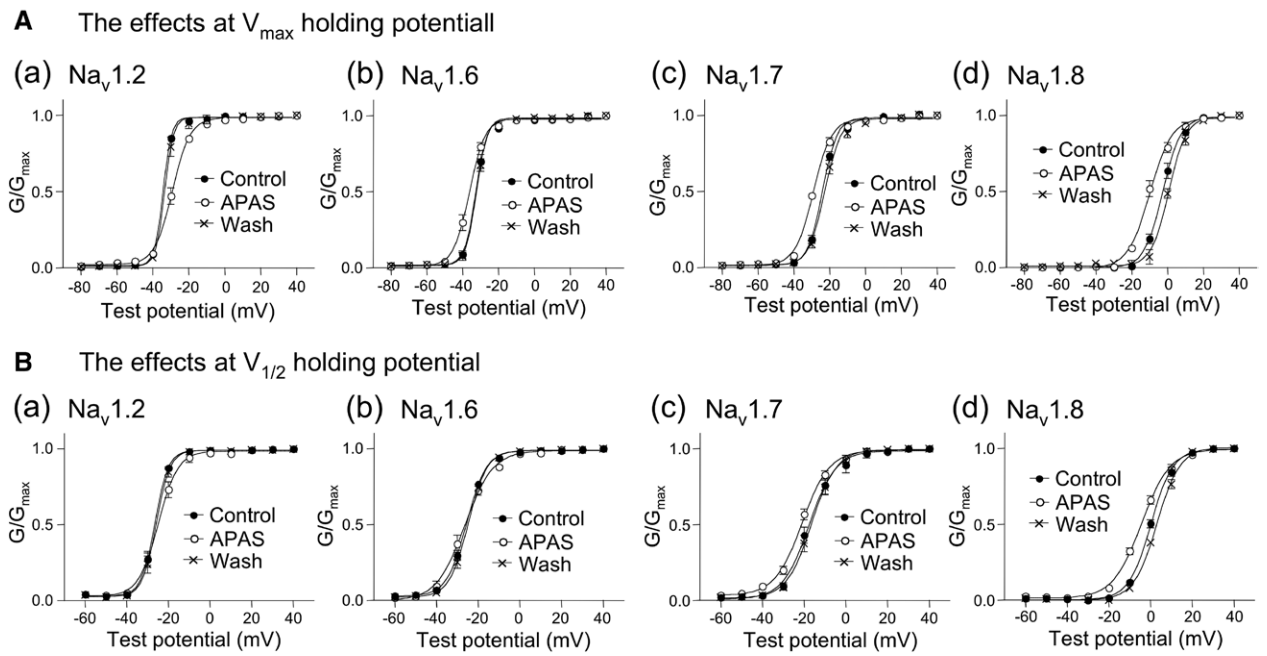

Fig. 6. Effects of allopregnanolone sulfate (APAS) on channel activation in oocytes expressing $Na_v1.2$ (*a*) (n = 5), $Na_v1.6$ (*b*) (n = 7), $Na_v1.7$ (*c*) (n = 5), or $Na_v1.8$ (*d*) (n = 6) α subunits with β_1 subunits from V_{max} (*A*) or $V_{1/2}$ holding potentials (*B*). *Closed circles*, *open circles*, and *cross* represent control, the effect of neurosteroids, and washout, respectively. Data are expressed as means ± SEM. Activation curves were fitted to the Boltzmann equation; $V_{1/2}$ is shown in table 2. Na_v = voltage-gated sodium channel; V_{max} holding potential = holding potential causing maximal current; $V_{1/2}$ holding potential = holding potential causing half-maximal current; Wash = washout.

Table 2. Effects of APAS on Activation and Inactivation

	$V_{1/2}$ (mV)					
	Holding V_{max}			Holding $V_{1/2}$		
	Control	APAS	Shift	Control	APAS	Shift
Activation						
$Na_v1.2$	−34.2 ± 0.5	−29.1 ± 1.0**	+5.1	−26.4 ± 0.8	−24.8 ± 1.1	+1.6
$Na_v1.6$	−32.5 ± 0.6	−36.3 ± 0.9***	−3.8	−25.6 ± 0.6	−26.7 ± 1.3	−1.1
$Na_v1.7$	−23.9 ± 0.6	−29.0 ± 0.3***	−5.1	−17.2 ± 1.7	−20.9 ± 0.9	−3.7
$Na_v1.8$	−2.7 ± 1.1	−9.8 ± 1.2***	−7.1	0.3 ± 0.6	−4.2 ± 0.8**	−4.5
Inactivation						
$Na_v1.2$	−50.1 ± 1.0	−58.1 ± 1.1***	−8.0			
$Na_v1.6$	−57.8 ± 0.5	−66.7 ± 0.7***	−8.9			
$Na_v1.7$	−72.3 ± 1.6	−79.0 ± 1.8***	−6.7			
$Na_v1.8$	−37.0 ± 2.2	−45.9 ± 1.7***	−8.9			

$V_{1/2}$ is calculated from nonlinear regression analyses of activation and inactivation curves shown in figures 6 and 7. Data are given as mean ± SEM; n = 5 ($Na_v1.2$), 7 ($Na_v1.6$), 5 ($Na_v1.7$), and 6 ($Na_v1.8$).

**P < 0.01; ***P < 0.001 compared with control, based on paired t test (two-tailed).

APAS = allopregnanolone sulfate; Holding V_{max} = holding potential causing maximal current; Holding $V_{1/2}$ = holding potential causing half-maximal current; Na_v = voltage-gated sodium channel; $V_{1/2}$ = the potential at which activation is half maximal for activation curve, and the voltage of half-maximal inactivation for inactivation curve.

Discussion

In the current study, we demonstrated that APAS and PAS differentially affected I_{Na} induced by four α subunits at both V_{max} and $V_{1/2}$ holding potentials. Moreover, we found that both neurosteroids suppress $Na_v1.2$, $Na_v1.6$, and $Na_v1.7$ at $V_{1/2}$ in a concentration-dependent manner. IC_{50} values indicated that the effect of APAS on $Na_v1.2$ was most potent among the two compounds and three α subunits. To the best of our knowledge, this is the first direct evidence of the various effects of these two neurosteroids on neuronal sodium channel α subunits. It is thought that APAS is synthesized from allopregnanolone by 3α-hydroxysteroid

Table 3. Effects of PAS on Activation and Inactivation

	$V_{1/2}$ (mV)					
	Holding V_{max}			Holding $V_{1/2}$		
	Control	PAS	Shift	Control	PAS	Shift
Activation						
$Na_v1.2$	−33.4 ± 0.6	−30.5 ± 1.5	+2.9	−26.1 ± 0.9	−23.7 ± 1.1**	+2.4
$Na_v1.6$	−32.1 ± 0.5	−32.4 ± 0.8	−0.3	−24.8 ± 0.8	−20.7 ± 1.4**	+4.1
$Na_v1.7$	−23.2 ± 0.5	−23.9 ± 0.6	−0.7	−18.7 ± 1.0	−18.0 ± 0.9	+0.7
$Na_v1.8$	−1.4 ± 2.1	−2.3 ± 1.7	−0.9	−0.2 ± 0.8	−1.1 ± 0.9	−0.9
Inactivation						
$Na_v1.2$	−49.9 ± 0.8	−54.4 ± 1.5**	−4.5			
$Na_v1.6$	−57.5 ± 0.5	−65.5 ± 0.5***	−8.0			
$Na_v1.7$	−72.3 ± 1.0	−78.9 ± 1.0***	−6.6			
$Na_v1.8$	−36.0 ± 1.3	−46.2 ± 1.4**	−10.2			

$V_{1/2}$ is calculated from nonlinear regression analyses of activation and inactivation curves (not shown). Data are given as mean ± SEM; n = 6 ($Na_v1.2$), 7 ($Na_v1.6$), 5 ($Na_v1.7$), and 6 ($Na_v1.8$).

** $P < 0.01$; *** $P < 0.001$ compared with control, based on paired *t* test (two-tailed).

Holding V_{max} = holding potential causing maximal current; Holding $V_{1/2}$ = holding potential causing half-maximal current; Na_v = voltage-gated sodium channel; PAS = pregnanolone sulfate; $V_{1/2}$ = the potential at which activation is half maximal for activation curve, and the voltage of half-maximal inactivation for inactivation curve.

sulfotransferase *in vivo*, because 3α-hydroxysteroid sulfotransferase has been isolated *in vivo*.[26] Therefore, allopregnanolone likely exerts a portion of its effects through APAS, which is its metabolite.

It was reported that the level of endogenous allopregnanolone changes in many physiological and pathological situations within a serum concentration range of 1 to 10 nmol/l.[27,28] However, it is not clear whether allopregnanolone has an analgesic effect in physiological concentrations. A recent study demonstrated that 1 and 10 μmol/l of allopregnanolone reduced mechanical allodynia and thermal heat hyperalgesia in normal and neuropathic pain models in rats after 10-μl intrathecal injection.[29] Another investigator reported that intrathecal administration of 10 μmol/l of allopregnanolone showed antihyperalgesic effects in hyperalgesic rats after spinal nerve ligation.[30] From these previous studies, concentrations approximately 1 μmol/l allopregnanolone at receptive fields are estimated to have an analgesic effect. In the current study, APAS tended to, *albeit* not significantly, suppress the I_{Na} of $Na_v1.2$ at 0.3 μmol/l by 8% and significantly ($P < 0.01$) inhibited it at 1 μmol/l by 19 ± 2%. The IC_{50} value of $Na_v1.2$ inhibition by APAS was 12 μmol/l. It was reported that relatively small degrees of sodium channel inhibition could have profound effects on the neuronal firing rate because a 10% inhibition of sodium current reduces the number of action potentials to 10 from a control response of 21 in 750 ms.[24] Therefore, APAS may reduce neuronal firing for $Na_v1.2$ at a concentration exhibiting the antinociceptive effects of allopregnanolone in animal models, whereas the effects of APAS and PAS on another three α and four α subunits, respectively, may not be pharmacologically relevant because these effects were observed at concentrations over 10 μmol/l. In addition, the effects of highly hydrophobic compounds—such as neurosteroids—we used tend to be attenuated in the voltage-clamp techniques with *Xenopus* oocytes, compared with the whole-cell voltage-clamp methods using mammalian cells. Indeed, it was reported that the enhancing effect by allopregnanolone on $GABA_A$ receptor combination ($\alpha_1\beta_2\gamma_{2L}$) was more potent in the human embryonic kidney 293 cells system (EC_{50}; 41 ± 2 nmol/l)[31] than that in the *Xenopus* oocyte system (EC_{50}; 177 ± 2 nmol/l).[32] This may be a limitation of experiments using the *Xenopus* oocyte expression system; this limitation indicates that APAS might inhibit function of $Na_v1.2$ more potently in a mammalian cell system than in the oocyte system, however, it also could potentiate $Na_v1.8$ function more potently in a mammalian cell. Therefore, further investigation is needed to consider the roles of these α subunits in humans.

Analysis of gating revealed common characteristics but also some differences in the effects of APAS and PAS on different α subunits. A common effect on all α subunits was enhancement of inactivation. Because of this enhancement effect, the inhibitions by two compounds at $V_{1/2}$ holding potentials could be interpreted as stronger effects because they shift inactivation curve to the hyperpolarizing direction, which makes the channel into further inactivated state. In contrast, APAS enhanced peak I_{Na} at V_{max}, shifted activation in the hyperpolarizing direction, and increased sodium currents in the hyperpolarizing range of the inactivation curves for $Na_v1.6$, $Na_v1.7$, and $Na_v1.8$. These changes indicate that APAS shifts channel gating equilibrium toward the open channel state and activates sodium channels. This action might attenuate the effects on the inactivated state and, especially, lead to enhancement of I_{Na} even in the inactivated state ($V_{1/2}$ holding potential) for $Na_v1.8$ in spite of the great enhancement of inactivation. However, for $Na_v1.2$, APAS profoundly suppressed peak I_{Na} at V_{max}, shifted activation in the depolarizing direction at V_{max}, and greatly decreased

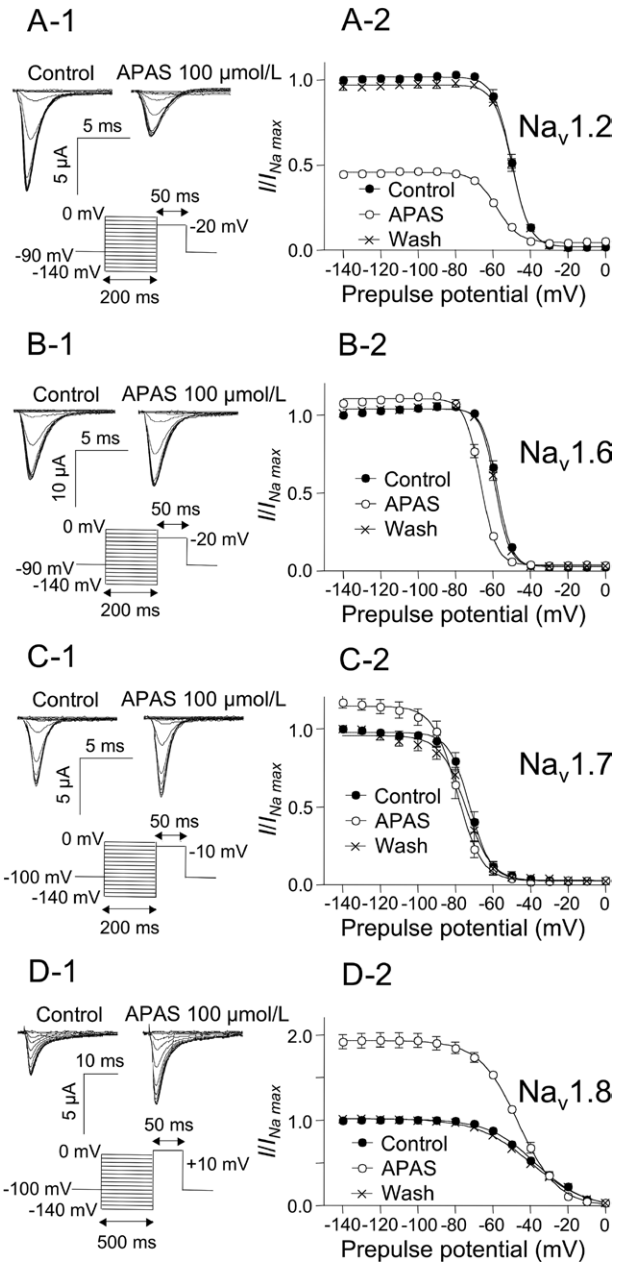

Fig. 7. Effects of allopregnanolone sulfate (APAS) on inactivation curves in oocytes expressing $Na_v1.2$ (*A*) (n = 6), $Na_v1.6$ (*B*) (n = 7), $Na_v1.7$ (*C*) (n = 5), or $Na_v1.8$ (*D*) (n = 6) α subunits with β_1 subunits. Currents were elicited by a 50-ms test pulse to –20 mV for $Na_v1.2$ and $Na_v1.6$, –10 mV for $Na_v1.7$, and +10 mV for $Na_v1.8$ after 200 ms (500 ms for only $Na_v1.8$) prepulses ranging from –140 mV to 0 mV in 10-mV increments from a V_{max} holding potential. Representative I_{Na} traces in both the absence and presence of APAS are shown in *A-1*, *B-1*, *C-1*, and *D-1*. Effects of APAS on inactivation curves (*closed circles*, control; open circles, neurosteroids; cross, washout) are shown in *A-2*, *B-2*, *C-2*, and *D-2*. Steady-state inactivation curves were fitted to the Boltzmann equation, and the $V_{1/2}$ values are shown in table 2. Data are expressed as means ± SEM. Na_v = voltage-gated sodium channel; Wash = washout.

sodium currents in the hyperpolarizing range of the inactivation curve, indicating that resting channel block is an important mechanism of APAS inhibition for only $Na_v1.2$. Both compounds demonstrated use-dependency for inhibition of $Na_v1.2$, $Na_v1.6$, and $Na_v1.7$, suggesting the ability to slow the recovery time from inactivation.[33] Many investigators have shown that sodium channel blockers, including local anesthetics, tricyclic antidepressants, and volatile anesthetics, enhance steady-state inactivation with no effect on activation and exhibit use-dependent block.[34–36] We demonstrated that APAS enhances inactivation and shows use-dependent block similar to other sodium channel blockers, yet it also has diverse effects on activation according to differences in α subunits. These actions suggest that APAS may have different binding sites or allosteric conformational mechanisms to change sodium channel function, although further investigation with site-directed mutagenesis is needed to rule out nonspecific membrane effects. PAS may have common binding sites with APAS, because it shows similar effects, although these changes were small.

The α subunit consists of four homologous domains (I to IV) containing six transmembrane segments (S1 to S6), and one reentrant P-region connecting S5 to S6 (SS1/SS2). Tetrodotoxin-sensitive α subunits, $Na_v1.2$, $Na_v1.6$, and $Na_v1.7$, are phylogenetically related and show 70 to 80% amino acid sequence identity. In contrast, tetrodotoxin-resistant α subunits, $Na_v1.8$, are phylogenetically distant and show only 55 to 56% sequence identity to the other three α subunits. In addition, the lengths of amino acid sequences of four α subunits differed within the range of 1957 to 2005 residues. Therefore, these differences would result in the diversity in neurosteroid action, especially in the effects on channel activation. Indeed, the longest extracellular regions in the α subunit (IS5 to SS1) are 93, 77, 73, and 66 amino acid residues in $Na_v1.2$, $Na_v1.6$, $Na_v1.7$, and $Na_v1.8$, respectively. The diversity in sequence and differences in the effects on activation according to α subunit may be important for clarifying binding sites and the mechanism of $Na_v1.2$ inhibition by APAS in further investigations.

γ-Aminobutyric acid type A receptors have been considered to be important for the analgesic effects of allopregnanolone because it has high potency as a positive $GABA_A$ modulator compared with other neurosteroids. Pregnanolone also affects $GABA_A$ receptors in a manner similar to that of allopregnanolone; nevertheless, its analgesic effect is weak. In fact, pregnanolone was shown to reduce mechanical allodynia without reduction of thermal heat hyperalgesia in a neuropathic pain model in contrast to attenuation of both by allopregnanolone.[28] The investigators suggested that the partial analgesic effects of pregnanolone are caused by suppression of glycine receptors by demonstrating that pregnanolone had a significant analgesic effect only in animals displaying a strychnine-induced allodynia in two types of allodynia models induced by bicuculline and strychnine.[28] Moreover, a recent report demonstrated that

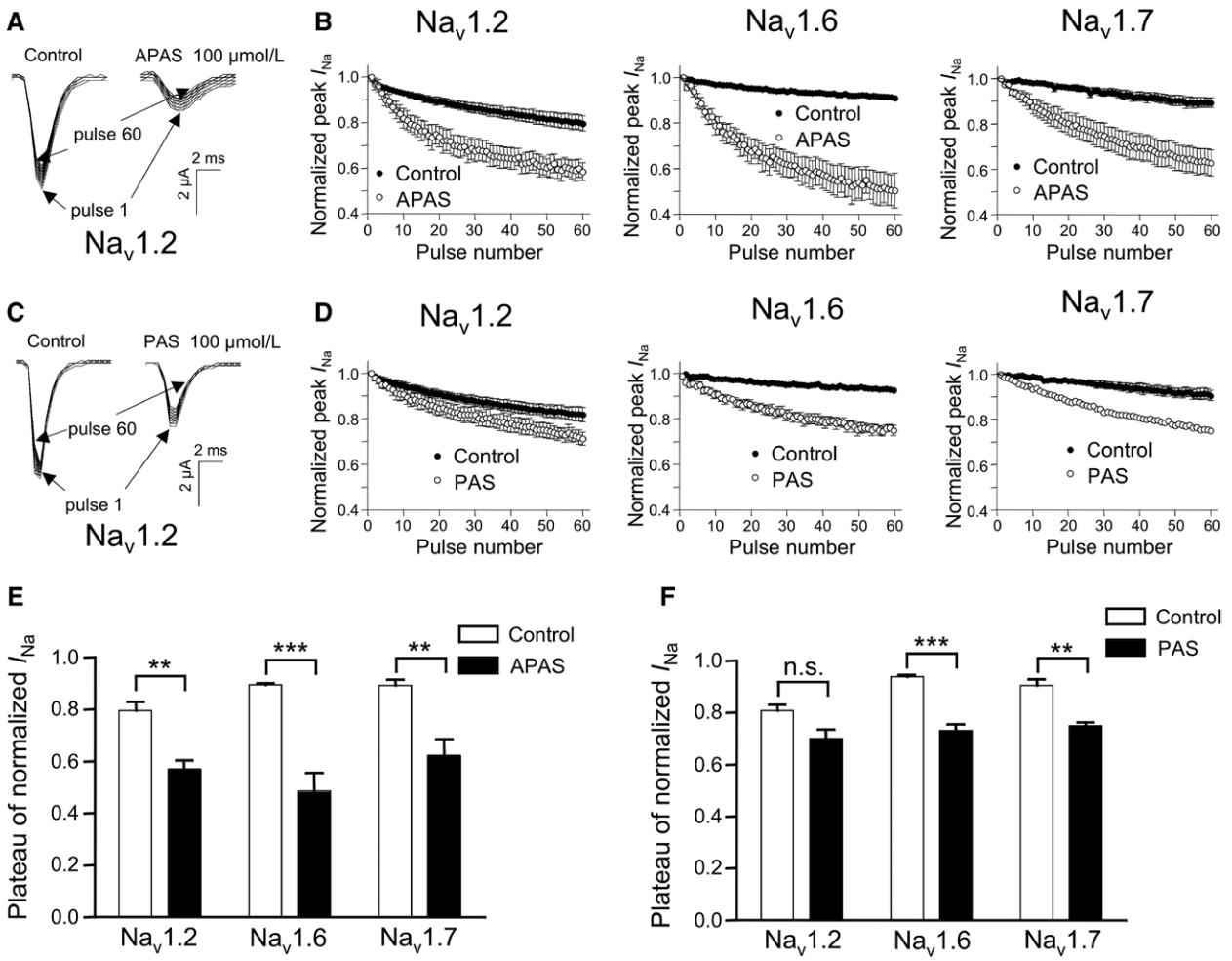

Fig. 8. Use-dependent blockage of sodium channels on Na$_v$1.2 (n = 5), Na$_v$1.6 (n = 6), and Na$_v$1.7 (n = 5) α subunits with β_1 subunits by allopregnanolone sulfate (APAS) and pregnanolone sulfate (PAS). Currents were elicited at 10 Hz by a 20-ms depolarizing pulse of –20 mV for Na$_v$1.2 and Na$_v$1.6 and –10 mV for Na$_v$1.7 from a $V_{1/2}$ holding potential in both the absence and presence of 100 μmol/l of the two compounds; representative I_{Na} traces in both the absence and presence of the two compounds (*A* and *C*). Peak currents were measured and normalized to the first pulse and plotted against the pulse number (*B*, the effects of APAS; *D*, the effects of PAS). *Closed circles* and *open circles* represent control and the effect of neurosteroids, respectively. Data were fitted to the monoexponential equation, and values for fractional blockage of the plateau of normalized I_{Na} are shown in *E* and *F*. Data are expressed as means ± SEM. $^{**}P < 0.01$ and $^{***}P < 0.001$ compared with the control, based on paired *t* test (two-tailed). Na$_v$ = voltage-gated sodium channel.

allopregnanolone shows analgesic effects in rats through suppression of T-type Ca^{2+} currents and potentiation of $GABA_A$ currents.[16] These previous reports indicate several mechanisms underlying the analgesic effect of allopregnanolone likely exist, as well as potentiation of $GABA_A$ receptors.

Sodium channel α subunits expressed in the dorsal root ganglion (Na$_v$1.7, Na$_v$1.8, and Na$_v$1.9) are thought to be involved in the pathogenesis of inflammatory and neuropathic pain. A recent study reported that Na$_v$1.2 also plays an important role in pain signaling. It was reported that Na$_v$1.2 and Na$_v$1.3 predominantly compose functional sodium channel currents within lamina I/II (dorsal horn) neurons, which mediate acute and chronic nociceptive signals from peripheral nociceptors to pain-processing regions in the brain.[37] Another recent report showed that mutations in Na$_v$1.2 are associated with seizures and pain characterized by headaches and back pain.[38] A disubstituted succinamide, a potent sodium channel blocker, was reported to attenuate nociceptive behavior in a rat model of tonic pain and was demonstrated to potently block Na$_v$1.2, as well as Na$_v$1.7 and Na$_v$1.8, with a potency two orders of magnitude higher than anticonvulsant and antiarrhythmic sodium channel blockers currently used to treat neuropathic pain.[39] Other investigators demonstrated that four sodium channel blockers, including lidocaine, mexiletine, benzocaine, and ambroxol, which are used clinically to treat pain, suppressed recombinant Na$_v$1.2 currents as well as tetrodotoxin-resistant Na^+ channel currents in rat sensory neurons, which comprised mostly Na$_v$1.8 currents. The authors suggested that these sodium channel blockers would induce analgesia according

to the amount of sodium channel blocking, including $Na_v1.2$ and $Na_v1.8$.[40] These recent reports support that suppression of $Na_v1.2$ function by APAS might be a mechanism underlying the analgesic effects of allopregnanolone.

In conclusion, APAS and PAS have diverse effects on $Na_v1.2$, $Na_v1.6$, $Na_v1.7$, and $Na_v1.8$ α subunits expressed in *Xenopus* oocytes, with differences in the effects on sodium channel gating. In particular, only APAS inhibited sodium currents of $Na_v1.2$ at pharmacologically relevant concentrations. These results raise the possibility that suppression of $Na_v1.2$ by APAS may be important for pain relief by allopregnanolone and provide a better understanding of the mechanisms underlying the analgesic effects of allopregnanolone. However, further studies are needed to clarify the relevance of sodium channel inhibition by APAS.

Acknowledgments

This study was supported by a Grant-in-Aid for Scientific Research from the Japan Society for the Promotion of Science, Tokyo, Japan (grant no. 21791480 to Dr. Horishita).

Competing Interests

The authors declare no competing interests.

Correspondence

Address correspondence to Dr. Horishita: Department of Anesthesiology, School of Medicine, University of Occupational and Environmental Health, 1-1 Isegaoka, Yahatanisiku, Kitakyushu 807–8555, Japan. thori@med.uoeh-u.ac.jp.

References

1. Baulieu EE: Neurosteroids: A novel function of the brain. Psychoneuroendocrinology 1998; 23:963–87
2. Compagnone NA, Mellon SH: Neurosteroids: Biosynthesis and function of these novel neuromodulators. Front Neuroendocrinol 2000; 21:1–56
3. Morrow AL: Recent developments in the significance and therapeutic relevance of neuroactive steroids—Introduction to the special issue. Pharmacol Ther 2007; 116:1–6
4. Brinton RD: Neurosteroids as regenerative agents in the brain: Therapeutic implications. Nat Rev Endocrinol 2013; 9:241–50
5. Majewska MD, Harrison NL, Schwartz RD, Barker JL, Paul SM: Steroid hormone metabolites are barbiturate-like modulators of the GABA receptor. Science 1986; 232:1004–7
6. Van Hemelrijck J, Muller P, Van Aken H, White PF: Relative potency of eltanolone, propofol, and thiopental for induction of anesthesia. ANESTHESIOLOGY 1994; 80:36–41
7. Zhu D, Wang MD, Bäckström T, Wahlström G: Evaluation and comparison of the pharmacokinetic and pharmacodynamic properties of allopregnanolone and pregnanolone at induction of anaesthesia in the male rat. Br J Anaesth 2001; 86:403–12
8. Kavaliers M, Wiebe JP: Analgesic effects of the progesterone metabolite, 3α-hydroxy-5α-pregnan-20-one, and possible modes of action in mice. Brain Res 1987; 415:393–8
9. Pathirathna S, Todorovic SM, Covey DF, Jevtovic-Todorovic V: 5α-Reduced neuroactive steroids alleviate thermal and mechanical hyperalgesia in rats with neuropathic pain. Pain 2005; 117:326–39
10. Ocvirk R, Pearson Murphy BE, Franklin KB, Abbott FV: Antinociceptive profile of ring A-reduced progesterone metabolites in the formalin test. Pain 2008; 138:402–9
11. Meyer L, Patte-Mensah C, Taleb O, Mensah-Nyagan AG: Allopregnanolone prevents and suppresses oxaliplatin-evoked painful neuropathy: Multi-parametric assessment and direct evidence. Pain 2011; 152:170–81
12. Kawano T, Soga T, Chi H, Eguchi S, Yamazaki F, Yokoyama M: The involvement of the neurosteroid allopregnanolone in the antihyperalgesic effect of paroxetine in a rat model of neuropathic pain. Neuroreport 2011; 22:984–8
13. Sasso O, Russo R, Vitiello S, Raso GM, D'Agostino G, Iacono A, Rana GL, Vallée M, Cuzzocrea S, Piazza PV, Meli R, Calignano A: Implication of allopregnanolone in the antinociceptive effect of *N*-palmitoylethanolamide in acute or persistent pain. Pain 2012; 153:33–41
14. Aouad M, Petit-Demoulière N, Goumon Y, Poisbeau P: Etifoxine stimulates allopregnanolone synthesis in the spinal cord to produce analgesia in experimental mononeuropathy. Eur J Pain 2014; 18:258–68
15. Jasmin L, Wu MV, Ohara PT: GABA puts a stop to pain. Curr Drug Targets CNS Neurol Disord 2004; 3:487–505
16. Pathirathna S, Brimelow BC, Jagodic MM, Krishnan K, Jiang X, Zorumski CF, Mennerick S, Covey DF, Todorovic SM, Jevtovic-Todorovic V: New evidence that both T-type calcium channels and $GABA_A$ channels are responsible for the potent peripheral analgesic effects of 5α-reduced neuroactive steroids. Pain 2005; 114:429–43
17. Kussius CL, Kaur N, Popescu GK: Pregnanolone sulfate promotes desensitization of activated NMDA receptors. J Neurosci 2009; 29:6819–27
18. Catterall WA: From ionic currents to molecular mechanisms: The structure and function of voltage-gated sodium channels. Neuron 2000; 26:13–25
19. Catterall WA, Goldin AL, Waxman SG: International Union of Pharmacology. XLVII. Nomenclature and structure-function relationships of voltage-gated sodium channels. Pharmacol Rev 2005; 57:397–409
20. Wood JN, Boorman JP, Okuse K, Baker MD: Voltage-gated sodium channels and pain pathways. J Neurobiol 2004; 61:55–71
21. Cummins TR, Sheets PL, Waxman SG: The roles of sodium channels in nociception: Implications for mechanisms of pain. Pain 2007; 131:243–57
22. Wang W, Gu J, Li YQ, Tao YX: Are voltage-gated sodium channels on the dorsal root ganglion involved in the development of neuropathic pain? Mol Pain 2011; 7:16
23. Horishita T, Ueno S, Yanagihara N, Sudo Y, Uezono Y, Okura D, Sata T: Inhibition by pregnenolone sulphate, a metabolite of the neurosteroid pregnenolone, of voltage-gated sodium channels expressed in *Xenopus* oocytes. J Pharmacol Sci 2012; 120:54–8
24. Horishita T, Eger EI II, Harris RA: The effects of volatile aromatic anesthetics on voltage-gated Na^+ channels expressed in *Xenopus* oocytes. Anesth Analg 2008; 107:1579–86
25. Scholz A, Kuboyama N, Hempelmann G, Vogel W: Complex blockade of TTX-resistant Na+ currents by lidocaine and bupivacaine reduce firing frequency in DRG neurons. J Neurophysiol 1998; 79:1746–54
26. Driscoll WJ, Martin BM, Chen HC, Strott CA: Isolation of two distinct 3-hydroxysteroid sulfotransferases from the guinea pig adrenal. Evidence for 3α-hydroxy *versus* 3 β-hydroxy stereospecificity. J Biol Chem 1993; 268:23496–503
27. Schlichter R, Keller AF, De Roo M, Breton JD, Inquimbert P, Poisbeau P: Fast nongenomic effects of steroids on synaptic

transmission and role of endogenous neurosteroids in spinal pain pathways. J Mol Neurosci 2006; 28:33–51

28. Mellon SH: Neurosteroid regulation of central nervous system development. Pharmacol Ther 2007; 116:107–24
29. Charlet A, Lasbennes F, Darbon P, Poisbeau P: Fast non-genomic effects of progesterone-derived neurosteroids on nociceptive thresholds and pain symptoms. Pain 2008; 139:603–9
30. Kawano T, Soga T, Chi H, Eguchi S, Yamazaki F, Kumagai N, Yokoyama M: Role of the neurosteroid allopregnanolone in the hyperalgesic behavior induced by painful nerve injury in rats. J Anesth 2011; 25:942–5
31. Akk G, Li P, Bracamontes J, Reichert DE, Covey DF, Steinbach JH: Mutations of the $GABA_A$ receptor α1 subunit M1 domain reveal unexpected complexity for modulation by neuroactive steroids. Mol Pharmacol 2008; 74:614–27
32. Lambert JJ, Belelli D, Harney SC, Peters JA, Frenguelli BG: Modulation of native and recombinant $GABA_A$ receptors by endogenous and synthetic neuroactive steroids. Brain Res Brain Res Rev 2001; 37:68–80
33. Wang GK, Russell C, Wang SY: State-dependent block of voltage-gated Na^+ channels by amitriptyline *via* the local anesthetic receptor and its implication for neuropathic pain. Pain 2004; 110:166–74
34. Ragsdale DS, McPhee JC, Scheuer T, Catterall WA: Molecular determinants of state-dependent block of Na^+ channels by local anesthetics. Science 1994; 265:1724–8
35. Poyraz D, Bräu ME, Wotka F, Puhlmann B, Scholz AM, Hempelmann G, Kox WJ, Spies CD: Lidocaine and octanol have different modes of action at tetrodotoxin-resistant Na^+ channels of peripheral nerves. Anesth Analg 2003; 97:1317–24
36. Ouyang W, Herold KF, Hemmings HC Jr: Comparative effects of halogenated inhaled anesthetics on voltage-gated Na^+ channel function. Anesthesiology 2009; 110:582–90
37. Hildebrand ME, Mezeyova J, Smith PL, Salter MW, Tringham E, Snutch TP: Identification of sodium channel isoforms that mediate action potential firing in lamina I/II spinal cord neurons. Mol Pain 2011; 7:67
38. Liao Y, Anttonen AK, Liukkonen E, Gaily E, Maljevic S, Schubert S, Bellan-Koch A, Petrou S, Ahonen VE, Lerche H, Lehesjoki AE: SCN2A mutation associated with neonatal epilepsy, late-onset episodic ataxia, myoclonus, and pain. Neurology 2010; 75:1454–8
39. Priest BT, Garcia ML, Middleton RE, Brochu RM, Clark S, Dai G, Dick IE, Felix JP, Liu CJ, Reiseter BS, Schmalhofer WA, Shao PP, Tang YS, Chou MZ, Kohler MG, Smith MM, Warren VA, Williams BS, Cohen CJ, Martin WJ, Meinke PT, Parsons WH, Wafford KA, Kaczorowski GJ: A disubstituted succinamide is a potent sodium channel blocker with efficacy in a rat pain model. Biochemistry 2004; 43:9866–76
40. Weiser T: Comparison of the effects of four Na^+ channel analgesics on TTX-resistant Na^+ currents in rat sensory neurons and recombinant $Na_v1.2$ channels. Neurosci Lett 2006; 395:179–84